

**AIAA Foundation Student Design Competition 2015/16**

**Undergraduate Individual – Aircraft**

**Conceptual Design of**

**TAJ PEGASUS**

**A Long Range Container Transportation Aircraft**

**Designer & Author : Waheedullah Taj**

## Signature Page

Designer and Author : Waheedullah Taj

Photo



AIAA Member ID : 513415

E-mail Address : waheedtaj@gmail.com

Date : 16 May 2016

Signature

A handwritten signature in blue ink, appearing to read 'Waheedullah Taj', written on a white background.

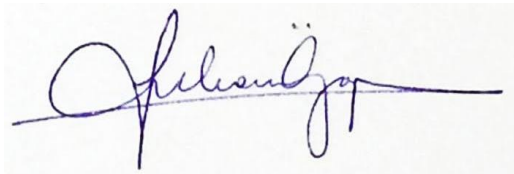
Faculty Advisor : Prof. Dr. Serkan Özgen

AIAA Member ID : 327810

E-mail Address : serkan.ozgen@ae.metu.edu.tr

Date : 16 May 2016

Signature

A handwritten signature in blue ink, appearing to read 'Serkan Özgen', written on a white background.

Copyright © 2016 by Waheedullah Taj

# Contents

CHAPTER 1 .....	6
1.1 Introduction .....	6
1.2 Design Method.....	7
1.3 Competitor Study.....	9
1.3.1 Performance Parameters .....	10
1.3.2 Geometric Characteristics.....	12
1.3.3 Design Characteristics .....	14
1.4 Conclusions .....	15
CHAPTER 2 .....	16
2.1 Concept 1 .....	17
2.2 Concept 2 .....	18
2.3 Concept 3 .....	19
2.1 Concept 4; The Final Configuration.....	20
CHAPTER 3 .....	21
3.1 Simple cruise mission profile .....	22
3.2 Estimation of the design take-off gross weight .....	22
3.3 Trade Studies .....	24
3.3.1 Payload Trade.....	24
3.3.2 Range Trade .....	25

3.3.3	Composite Materials Trade.....	25
CHAPTER 4	.....	27
4.1	Airfoil Selection .....	28
4.2	Other Wing Properties.....	29
CHAPTER 5	.....	31
5.1	Power-to-Weight Ratio .....	31
5.2	Wing Loading .....	33
5.2.1	Cruise .....	33
5.2.2	Climb Rate .....	34
5.2.3	Takeoff Distance.....	34
5.2.4	Landing Distance .....	35
5.2.5	Service Ceiling .....	35
5.2.6	Conclusions .....	36
CHAPTER 6	.....	37
6.1	Empty Weight Fraction .....	37
CHAPTER 7	.....	39
7.1	Fuel Volume .....	39
7.2	Wing Sizing and Planform Shape .....	40
7.3	Fuselage Length .....	41
7.4	Tail Sizing and Planform Shape .....	41

7.4.1	Tails .....	42
7.5	Engine and Propeller Dimensions and Weight .....	43
CHAPTER 8 .....		44
8.1	Weights of Major Components.....	44
8.2	Landing Gear Placement and Sizing .....	46
CHAPTER 9 .....		49
9.1	Lift Curve Slope .....	49
9.2	Drag.....	52
CHAPTER 10 .....		53
10.1	Power Curves .....	53
10.2	Takeoff And Landing Distances .....	56
CHAPTER 11 .....		57
CHAPTER 12 .....		65
12.1	Stability and Control .....	65
12.1.1	CG Envelope .....	65
12.1.2	Control Surfaces.....	67
12.1.3	Stability Derivatives.....	68
12.2	Handling the Payload .....	71
12.2.1	Attachment Mechanism.....	71
12.2.2	Gates .....	71

12.3	Crew Station Design .....	73
12.4	Air Loads and Structures .....	74
12.4.1	Wings.....	76
12.4.2	Empennage .....	77
12.4.3	Fuselage .....	78
12.5	Materials Selection .....	78
12.5.1	Wings.....	79
12.5.2	Fuselage .....	80
12.5.3	Tails .....	80
CHAPTER 13	.....	84
REFERENCES:	.....	92

# CHAPTER 1

## Design Basics

---

“When once you have tasted flight, you will forever walk the earth with your eyes turned skyward, for there have you been, and there you will always long to return.”

Leonardo da Vinci

### 1.1 INTRODUCTION

There is a need for a new military aerial transport vehicle that can swiftly pick up 20 ft. containers and deliver them to war zones. The containers could contain first aid, military equipment and others. The aircraft sought should have among other qualities, the ability to fly without the container and drop the container mid-air. It should also takeoff and land on rough surfaces. This document reports the procedures undertaken while designing Taj Pegasus, a transport aircraft that meets the above criteria.

Taj Pegasus is a high aspect ratio conventional aircraft with conventional tail designed as a response to the Request for Proposal published by American Institute of Aeronautics and Astronautics Foundation for the 2015/16 Undergraduate Individual Aircraft Design Condition. It meets all the requirements set forth by the Request for Proposal.

### 1.2 REQUIREMENTS

The design is performed as per requirements of 2015/16 Undergraduate Individual Aircraft Design Competition of American Institute of Aeronautics and Astronautics (AIAA) Foundation. The containers to

be carried with the airplane have an empty weight of 5140 lb. and a payload of up to 40000 lb. and have to be carried external to the aircraft. The aircraft should be able to fly without the container and drop the container when desired. For maintenance purposes the aircraft should use the same engine and the propellers as Lockheed Martin C130H, i.e. Rolls Royce Allison T-56-A-15 engines and NP2000 propellers by Hamilton Sunstrand. The rest of the requirements are summarized below.

- Crew: 3 people.
- Cruise speed: at least 250 knots at an altitude of 23000 ft.
- Payload: 45140 lb. (Container + Contents).
- Service Ceiling: 33000 ft. with container empty.
- Rate of climb: 1500 ft/min at an altitude of 10000 ft.
- Takeoff and Landing Distances: 3500 ft. (both).
- Range: 1000 nm.

The engine and the propeller have the following properties:

- Uninstalled Takeoff Power: 4300 shp.
- Takeoff Specific Fuel Consumption: 0.5 lbs/hp/hr.
- Propeller Efficiency: 0.9.

## 1.3 DESIGN METHOD

This report utilizes the design method of Daniel Raymer outlined in [1]. The design starts with an initial weight estimate which is a result of considering both competitor aircraft and statistical equations. This estimate is used to design the wings and decide on critical performance parameters such as power to weight ratio and wing loading. The weight is then estimated once again. This estimate is considered to be more accurate because in this estimate the effect of more parameters on the aircraft weight are



considered than before. Later geometric characteristics of the aircraft are decided upon and the weight and center of gravity of the aircraft are estimated once again, this time using component buildup method. Next aerodynamic characteristics of the whole airplane are calculated and the performance of the aircraft is compared against the requirements. Finally carpet plots are obtained and power and wing loading levels are optimized to meet the requirements with minimal weight. Various aspects of the design like stability and control, structures, certification and others are considered and explained in detail.

All the equations used throughout this design were programmed into a Ms. Excel file. This is very important because mistakes in calculations can easily be detected and optimization process is completely automated when the design is programmed into the computer.

Drawings of the aircraft were prepared at various stages of the design. At the initial stages the drawings were prepared in a software named OpenVSP. This software is easy to use but it does not allow full control over the design. At the later stages however, SolidWorks was used to draw the 3D model of the aircraft.

## 1.4 MISCELLANEOUS

### 1.4.1 Units

Conventionally aircraft designers have used imperial units in the design procedure. It is also customary to use Knots (indicated by kts. In this report) and miles per hour (Mhp) for speed and nautical miles (nmi.) for distance from time to time. Most aircraft design books and the tools and figures in them are thus constructed using these units. Hence this report will continue this custom. Imperial units will be used virtually throughout the design. Knots, Miles per hour and nautical miles will be used to replace feet per second and feet when necessary.

### 1.4.2 Atmospheric Data

Various atmospheric data such as density and local speed of sound at different altitudes were needed throughout the design. All such data were readily obtained from [2]. This is a very useful and handy tool and the author suggests every aircraft designer to have this tool bookmarked in his/her web browser.

## 1.5 COMPETITOR STUDY

Airplane design is an evolutionary, rather than revolutionary, process. Which means a lot can be learned from studying aircraft of the same category when designing a new aircraft. Some important characteristics of aircraft similar in role, payload and range to the requirements were compiled. The following data is compiled from [3], [4], [5], [6], [7], [8], [9], [10], [11] and [12]. These tables will be used throughout the design process for reference and comparison.

### 1.5.1 Performance Parameters

Design Requirements		Alenia C-27	Embraer KC-390	Lockheed Martin C-130J	Shaanxi Y-9
<b>Crew</b>	3	3	2	3	3-4
<b>Cruise Speed (kts)</b>	250 kts @ 23000 ft. with max load	240	460	330	351
<b>Service Ceiling (ft.)</b>	33000 ft. (empty container)	25000	36000	30560	34120
<b>Rate of Climb (ft/m)</b>	1500 ft/m @ 10000 ft	1000	N/F	1500	N/F
<b>Take-off distance (ft.)</b>	3500 ft	2300	N/F	3127	4430
<b>Range (nm)</b>	1000	2500	1400	2835	3700
<b>Payload (lb.)</b>	45140 (max)	25353	52029	44000	55000

Antonov An-12	Fairchild C-123 K	Transall C-160	Kawasaki C-1	HAL IL-214	Shaanxi Y-8 (F-100)
5	4	3	5	3	2-5
310	198	260	235	437	350
33000	29000	27000	38000	42979	34120
1000	1220	1000	3500	N/F	1552
2300	N/F	N/F	N/F	3440	4170
2100	1278	2500	700	1775	3489
44000	24000	35275	31910	44000	44090

*Table 1: Design requirements and competitor aircraft performance. Note: N/F stands for “Not Found”.*

**1.5.1.1 Remarks:**

- Among the competitor aircraft that were chosen for consideration in this study, Fairchild C-123 K has a relatively poor performance. This is due to the fact that Fairchild C-123 K is a relatively old aircraft compared to the others and uses inferior technology. Thus this aircraft will be mostly ignored when using competitor data.

## 1.5.2 Geometric Characteristics

<b>Geometric Characteristics</b>	<b>Alenia C-27</b>	<b>Embraer KC-390</b>	<b>Lockheed Martin C-130J</b>	<b>Shaanxi Y-9</b>	<b>Antonov An-12</b>
<b>Length (ft.)</b>	74.5	111.3	97.8	118.1	108.6
<b>Wing Span (ft.)</b>	94.2	115.0	132.5	124.7	124.7
<b>Wing Area (ft<sup>2</sup>)</b>	882.6	1507.0	1745.0	1312.1	1310.0
<b>Aspect Ratio</b>	10.0	N/F	10.1	11.9	N/F
<b>Propeller Diameter (ft.)</b>	13.5	N/F	13.5	14.8	N/F
<b>Height (ft.)</b>	32.2	33.7	38.7	37.0	34.5
<b>Wing Position</b>	High Wing	High Wing	High Wing	High Wing	High Wing
<b>Tail Configuration</b>	Regular tail	T-tail	Regular tail	Regular tail	Regular tail
<b>Empty Weight (lb.)</b>	37480	N/F	75562	85980	62000
<b>Design TO weight (lb.)</b>	67240	N/F	164000	169755	122000

<b>Fairchild C-123 K</b>	<b>Transall C-160</b>	<b>Kawasaki C-1</b>	<b>HAL IL-214</b>	<b>Shaanxi Y-8</b>	<b>Averages</b>
75.8	106.3	95.1	125.4	111.6	<b>102.5</b>
110.0	131.2	100.4	116.5	124.7	<b>117.4</b>
1222.8	1722.2	1297.0	N/F	1312.1	<b>1231.0</b>
N/F	N/F	N/F	N/F	11.9	<b>10.98</b>
N/F	N/F	N/F	N/F	14.8	<b>14.2</b>
34.1	38.4	32.8	42.5	36.6	<b>36.0</b>
High Wing	High Wing	High Wing	High Wing	High Wing	-
Regular tail	Regular tail	T-tail	T-tail	Regular tail	-
35366	63935	53410	N/F	76060	<b>61224.1</b>
60000	112435	85300	149915	134480	<b>106512.5</b>

Table 2: Some geometric characteristics of competitor aircraft. Note: N/F stands for "Not Found".

**1.5.2.1 Remarks:**

- All of the competitor aircraft shown in Table 2 use high wing configuration.
- Conventional tail configuration seems to dominate the market in this aircraft category.

### 1.5.3 Design Characteristics

Design Characteristics	Alenia C-27	Embraer KC-390	Lockheed Martin C-130J	Shaanxi Y-9	Antonov An-12
<b>W/S (lb/ft<sup>2</sup>)</b>	76.2	108.3	94.0	129.4	92.7
<b>P/W (hp/lb)</b>	0.138	N/A	0.112	0.120	0.132
<b>T/W (lb-force/lb)</b>	N/A	N/A	N/A	N/A	N/A
<b>W<sub>e</sub>/W<sub>0</sub></b>	0.557	N/F	0.461	0.506	0.508
<b>W<sub>i</sub>/W<sub>0</sub></b>	0.319	0.505	0.280	0.299	0.399
<b>Stall Speed (ft/s)</b>	176.8	N/F	168.6	N/F	N/F
<b>Top speed (mph)</b>	374	528	416	403	483

Fairchild C-123 K	Transall C-160	Kawasaki C-1	HAL IL- 214	Shaanxi Y-8	Averages
49.1	65.3	65.8	N/F	102.5	<b>87.0</b>
0.083	0.109	N/A	N/A	0.125	<b>0.117</b>
N/A	N/A	0.340	0.459	N/A	<b>0.4</b>
0.498	0.589	0.626	N/F	0.566	<b>0.539</b>
N/F	0.259	N/F	0.199	0.376	<b>0.330</b>
N/F	161.3	N/F	N/F	N/F	<b>168.9</b>
228	319	500	540	410	<b>420.1</b>

*Table 3: Some design characteristics of competitor aircraft. Note: N/F stands for “Not Found” and N/A stands for “Not Applicable”.*

#### **1.5.3.1 Remarks:**

- For some aircraft design take-off weight could not be found. As a result, maximum take-off weight was used in calculation of  $W/S$ ,  $P/W$ ,  $T/W$ ,  $W_e/W_0$  and  $W_f/W_0$ .

## **1.6 CONCLUSIONS**

The airplanes considered in this chapter have somewhat similar characteristics. For example the average aspect ratio is 10.98 and little deviation from that value is observed. Similarly most airplanes considered use high wing and conventional tail configurations. These will be helpful when deciding on different characteristics of Taj Pegasus. For example aspect ratio of Taj Pegasus was directly chosen to be 10.98 based on this competitor study.



# CHAPTER 2

## System Level Concepts; Trade and Selection

---

“Simplicity is the ultimate form of sophistication.”

Leonardo da Vinci

Many different concept aircraft were considered before and during the design procedure. While these alternatives offered many advantages, they were not feasible in some other aspects. Four of the most important alternative concepts considered, benefits of using them, and the reason why they were dismissed are discussed below. This part also intends to explain why each of the choices were made for the final configuration.

## 2.1 CONCEPT 1

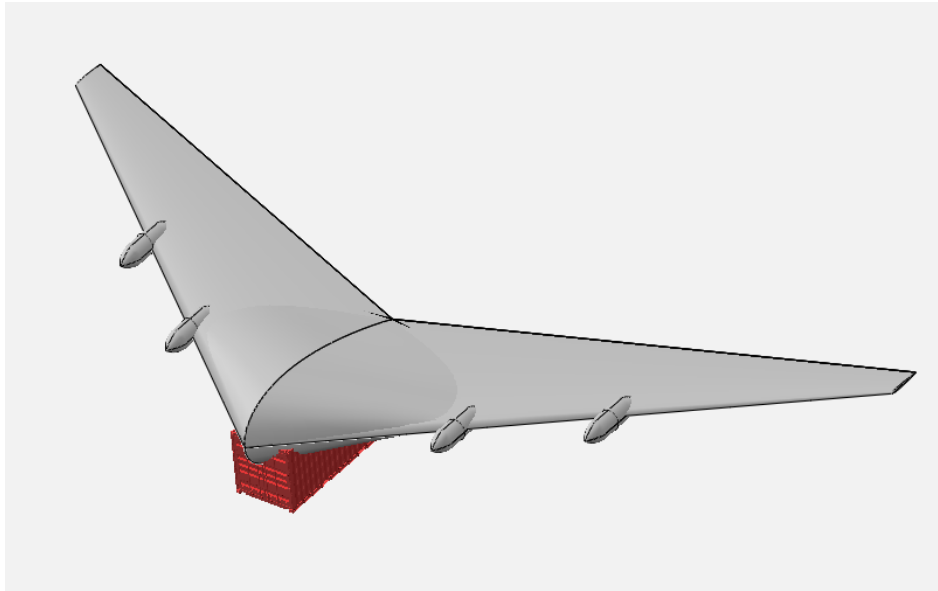


*Figure 1: Concept 1; a flying wing airplane.*

Concept 1 was a flying wing airplane and it was the runner-up in the final concept selection. The payload of Taj Pegasus is only one 20 ft. container. This means a long fuselage is not necessary and a flying wing airplane such as that shown in Figure 1 would be a very wise choice in terms of weight and drag since it does not have tails or a distinct fuselage. Using a flying wing would have had other advantages too. Since the container is attached directly to the wings (which are already very strong) additional structural stiffeners in the fuselage would be avoided.

However this concept was considered unfeasible because of two major reasons. First flying wings need to have great sweep angles in order to eliminate the need for the tail. Wings with high sweeps do not generate much lift unless the aircraft flies at very high velocities, i.e. near Mach 1 while Taj Pegasus is intended to fly at much lower velocities.

Second, this concept would be an inherently unstable aircraft and this is highly undesirable in transport category aircraft.

## 2.2 CONCEPT 2

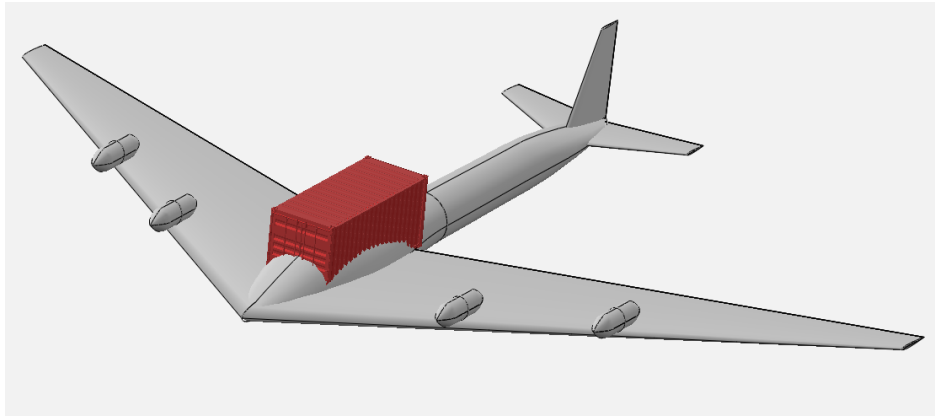


*Figure 2: Concept 2; a low wing configuration.*

The second concept was a low wing aircraft with a flat fuselage very near the ground. This aircraft would have a hole in the middle where the container stands. The concept has a positive dihedral for enhanced stability. The pilot and copilot are in the nose which is located in front of the container. The tail could have been a T-tail, a conventional tail or a boom mounted tail. The engines are on top of the wings to avoid contact with the ground. One of the greatest problems faced during the design of Taj Pegasus was the landing gear design. Landing gears either have to be excessively long, making them very heavy, or very large external canopies have to be designed in order to house and support the landing gears which adds to the weight and drag of the aircraft. Since both the wing and fuselage of Concept 2 are very close to the ground very light and effective landing gears could have been designed.

The main disadvantage of Concept 2 is that loading and unloading would have been very difficult with this configuration. The RFP explicitly states that the loading procedure has to be swift. However if this concept was used the container would have to be loaded with a crane or similar mechanisms. Similarly dropping the container would have to be done using complex mechanisms and maneuvers.

## 2.3 CONCEPT 3

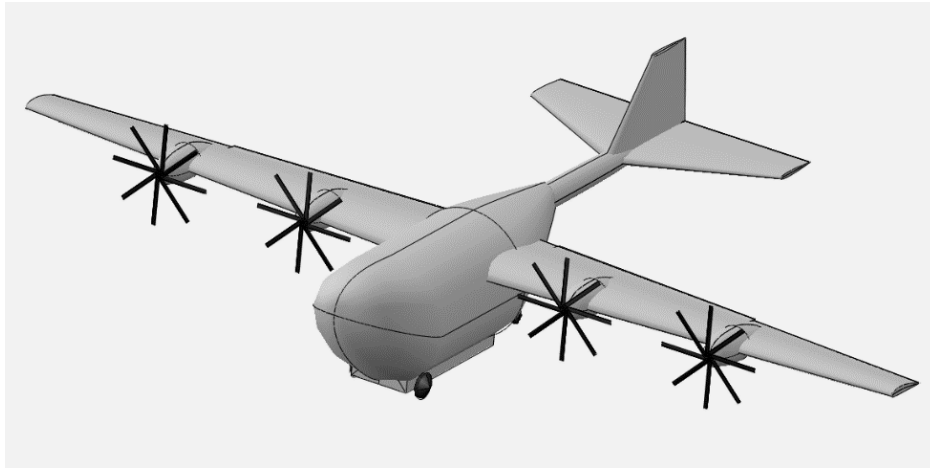


*Figure 3: Concept 3; high wing configuration with gates at the front.*

Concept 3 is very similar to the final configuration. The major difference between this concept and the final configuration is that in this concept the front of the fuselage, rather than the back is opened when loading and unloading the container. This concept uses a tail dragger landing gear configuration.

The greatest advantage of this concept is that it makes loading and unloading the container easy. The loading procedure does not require a truck, neither does it require the pilots to move the aircraft in reverse. The airplane can move forward to the point where the container is stationed and attach the container to its payload compartment.

There are many disadvantages to this concept. First of all the fuselage has to be very bulky and large. This directly increases weight and drag of the airplane. Secondly, dropping the container with this configuration is risky because if released while flying, the container has a tendency to go backwards. This would cause the container to crash to the cone shaped rear half of the fuselage. Last but not least it would be near impossible for the aircraft to fly without a container. The void where the container stands would create immense amounts of drag when the container is absent.

## 2.1 CONCEPT 4; THE FINAL CONFIGURATION

At the end all these concepts converged to the final configuration that is designed in this report. The final configuration is a high wing, high aspect ratio and highly conventional airplane that has a conventional tail. The engines are below the wing, the container is hung below a narrow fuselage and streamlined surfaces cover both the front and the rear of the fuselage. Three sides of the fuselage are directly exposed to the free stream because the RFP requires that the container be carried externally. The aircraft uses a tricycle landing gear with nose landing gear directly beneath the cockpit and main landing gears are stationed in the wings. A 3D drawing of the final configuration is shown below. This design is stable, compact, and reliable. The aircraft can be manufactured easily because its structural members are made of simple shapes only.

The aircraft has a high aspect ratio which improves aerodynamic performance of the aircraft. This reduces fuel consumption and greenhouse gas emissions thus contributing to a healthier environment.

Last but not least this design is aesthetically pleasing which adds to its social acceptance. This is important because history has shown that a better performing aircraft might lose to an aircraft of inferior performance in bids if the latter is more beautiful.



*Figure 4: The final configuration of Taj Pegasus.*

# CHAPTER 3

## Initial Sizing

---

“Aeronautics was neither an industry nor a science. It was a miracle.”

Igor Sikorsky

### 3.1 INTRODUCTION AND OBJECTIVES

This chapter aims to establish a weight estimate of Taj Pegasus using the information known about Taj Pegasus from the RFP or other sources. At the end of this chapter an approximation of empty weight, crew weight, total fuel weight, fuel weight spent at each flight segment, and design takeoff weight of Taj Pegasus will be obtained. A trade study will also be performed to observe the effects of changing some requirements on the aircraft weight.

The weight estimation method used in this chapter uses statistics and some empirical equations. Crew weight and payload were guessed based on common sense and obtained directly from the RFP, respectively. The empty weight and fuel weight were calculated as fractions of design takeoff weight. Empty weight fraction estimation takes one input only, which is aircraft category (transport, fighter, trainer etc.). The results, though crude in nature, are deemed accurate enough for this stage of the design. Fuel weight fraction was estimated based on the amount of fuel spent in every flight segment. Fuel weight fraction of some flight segments were again substituted from historical data, while some others were calculated using mathematical equations with some minor assumptions.

### 3.2 SIMPLE CRUISE MISSION PROFILE

The cargo aircraft described in AIAA design competition has to take-off and fly to a distance of 1000 nautical miles with full payload. The figure below describes this flight envelope graphically.

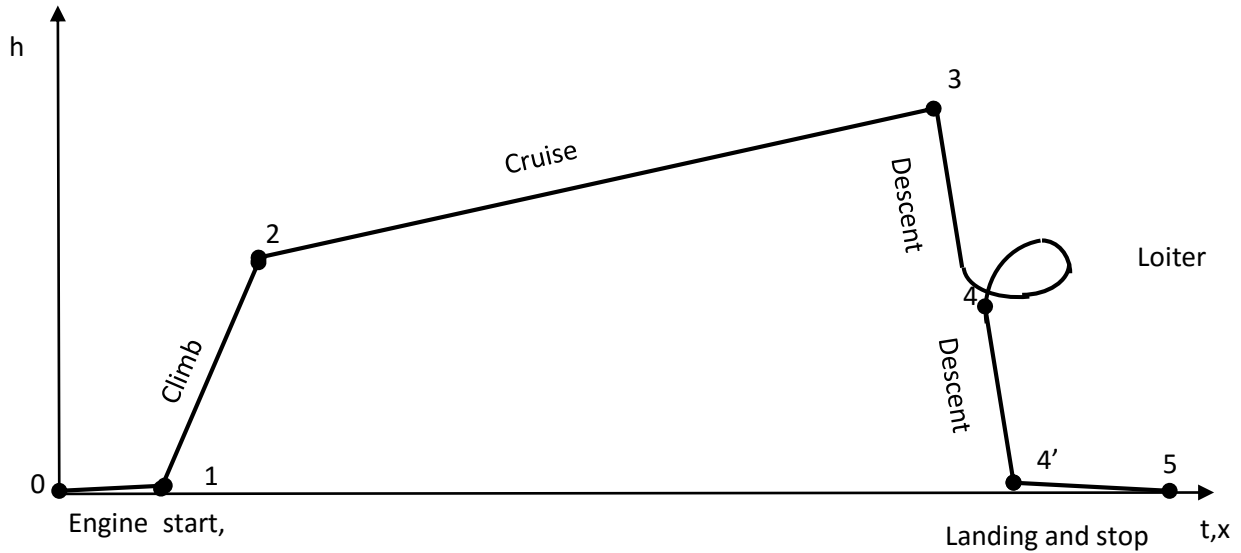


Figure 5: Simple cruise mission profile of TAJ PEGASUS.

Where h shows altitude, t shows time and x shows forward distance. The distances in the figure are for demonstration purposes only and they are not to be scaled.

### 3.3 ESTIMATION OF THE DESIGN TAKE-OFF GROSS WEIGHT

Design gross weight,  $W_0$ , is made up of four parts; crew weight,  $W_c$ , payload weight,  $W_p$ , fuel weight,  $W_f$  and empty weight,  $W_e$ .

$$W_0 = W_c + W_p + W_e + W_f \quad \text{or} \quad W_0 = \frac{W_c + W_p}{1 - \frac{W_e}{W_0} - \frac{W_f}{W_0}} \quad (1)$$

The crew of 3 people was estimated to weigh about 600 lb. The payload of Taj Pegasus is a container weighing a maximum of 45140 lb. Empty weight fraction for a cargo bomber is statistically given by [1].

$$\frac{W_e}{W_0} = 0.93W_0^{-0.07} \quad (2)$$

Fuel consumption will be calculated as mission segment fuel weight fractions and then multiplied together to receive overall fuel spending. The subscripts seen here show the stations in Figure 5.

$$\frac{W_5}{W_0} = \frac{W_5}{W_4} \frac{W_4}{W_3} \frac{W_3}{W_2} \frac{W_2}{W_1} \frac{W_1}{W_0} \quad (3)$$

Mission segment fuel weight fraction from instant 0 to instant 1 and from instant 1 to 2 will be assumed to be 0.97 and 0.985 respectively based on historical figures given by [1].

For calculating mission segment fuel weight fraction from instant 2 to 3, Brequet range equation was used [1]

$$\frac{W_3}{W_2} = \exp\left(\frac{-RC}{V_\infty \bar{D}}\right) = 0.905 \quad (4)$$

Here range, R, and cruise velocity,  $V_\infty$ , were directly substituted from the requirements. Specific fuel consumption at the cruise altitude was decreased due to density drop by using the sizing equations provided in [13] and found to be  $C = 0.426$  lbs/hr/hp. Lift to drag ratio, L/D, was estimated to be 17 based on aspect ratio and wetted area ratio and using figures provided in [1].

Mission segment fuel weight fraction for loiter from instant 3 to 4 can be calculated from endurance version of Eq. ( 4 ). A loiter time of 20 min = 1200 s will be allocated [14]. Propeller airplanes fly with a lower lift to drag ratio in loiter, thus  $L/D = 14.722$  [1]. Then  $W_4/W_3 = 0.989$ .

For descent, landing and stop, (4-5) historical trends were used again, hence  $W_5/W_4 = 0.995$  [1]. Then  $W_5/W_0 = 0.85$  and  $W_f/W_0 = 0.159$  allowing about 6% reserve fuel.

Finally from Eq. ( 1 )  $W_0 = 106914.5$  lb. and  $W_e/W_0 = 0.414$



# 3.4 TRADE STUDIES

## 3.4.1 Payload Trade

The figure below shows how the design empty weight of the aircraft changes with changing payload.

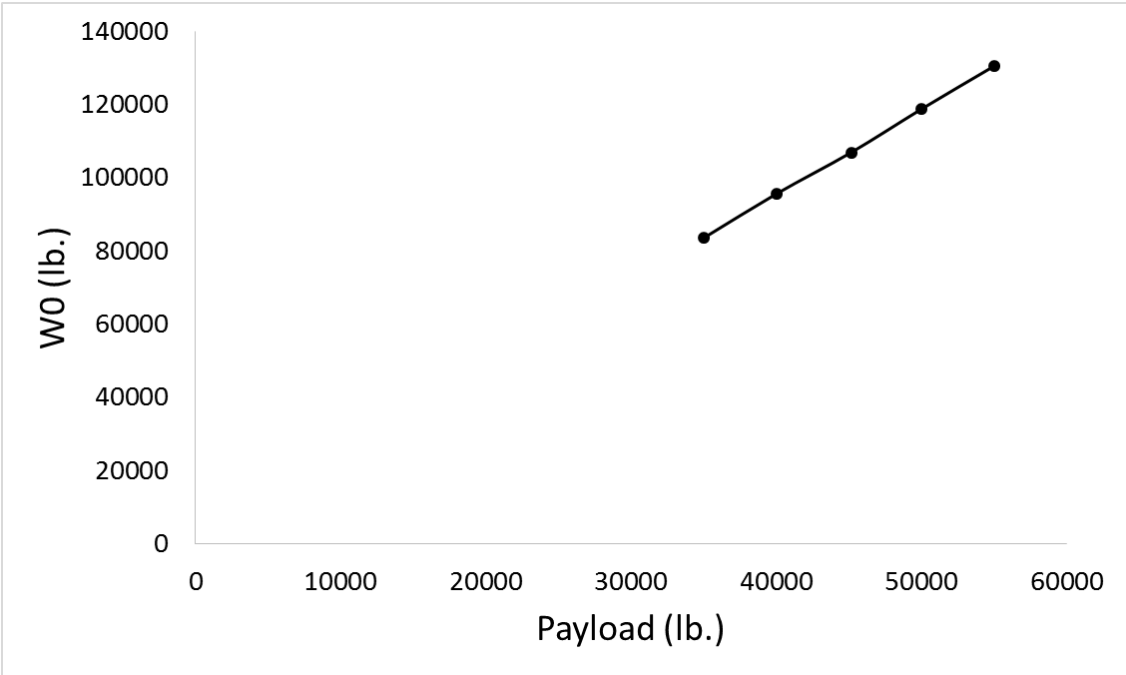


Figure 6 plot of design gross weight versus payload weight.

### 3.4.2 Range Trade

The scatter below shows how design gross weight of the aircraft changes with changing range

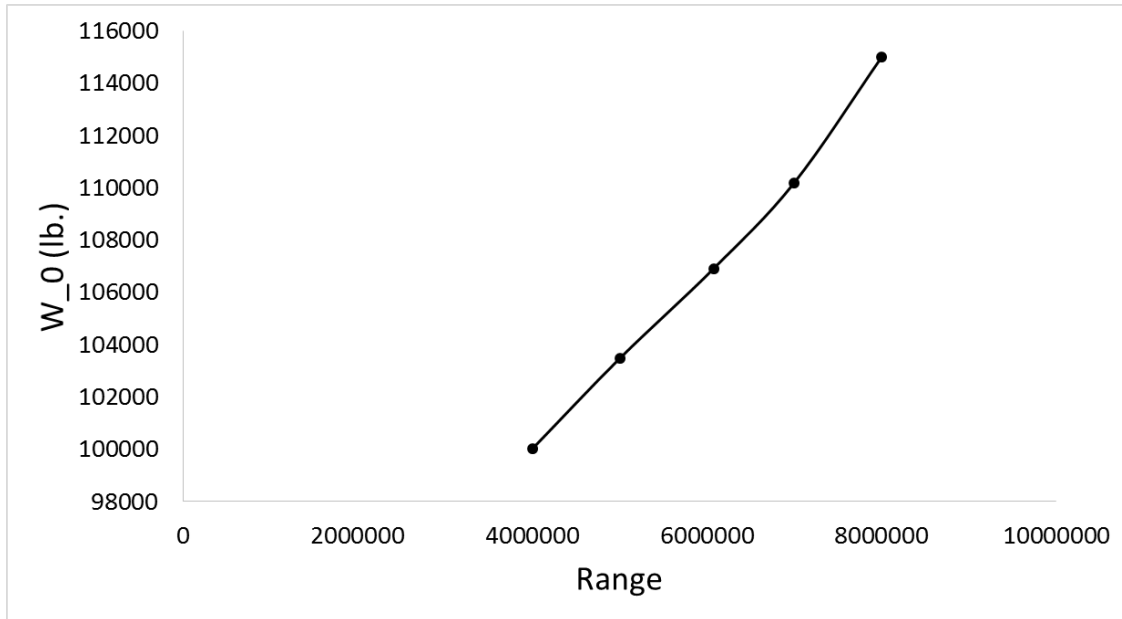


Figure 7 Plot of design gross weight versus range. Note that range is given in ft.

### 3.4.3 Composite Materials Trade

According to statistical data given by [1] the empty weight fraction of the aircraft decreases by 5% if it is made of composite materials. The table and scatter below show how the gross weight of the aircraft changes if the aircraft is mostly made of composite materials rather than metals.

Material	W <sub>0</sub> (lb.)	W <sub>e</sub> (lb.)
Metals	106914.5269	44206.59827
Composites	102265.3463	42416.07196

Table 4 Change in design take-off weight of the aircraft if it was made of composites or metals mostly.

## 3.5 CONCLUSIONS

Taj Pegasus was estimated to weigh 106914.5 lb. This weight could change significantly if the customer decided to change the requirements or if the aircraft is manufactured from composites. For example if reducing the payload weight from 45140 lb. to 40000 lb. alone could reduce aircraft design takeoff weight to around 85000 lb. Which means huge savings in production, operating and maintenance costs.

# CHAPTER 4

## Airfoil Selection and Wing Design

---

“There is no flying without wings.”

French proverb

### 4.1 INTRODUCTION AND OBJECTIVES

This chapter is concerned with designing or selecting a good airfoil for Taj Pegasus and determining some important features of the wings. The design of actual dimensions and shape of the wing is left for later.

The airfoil could be selected on based on different segments of flight depending on the type of the aircraft. Since this is a transport aircraft and spends most of its operating life in cruise the airfoil is selected based on this flight segment. A list of candidate airfoils were prepared after considering some threshold criteria and the best of the candidate airfoils were selected as the final choice. When choosing the final airfoil many different characteristics of the airfoil such as maximum coefficient of lift, minimum coefficient of drag, coefficient of pitching moment at zero angle of attack and the behavior of pitching moment at the stall region were considered.

## 4.2 AIRFOIL SELECTION

There are two main parameters used in airfoil selection. These are design lift coefficient, that is, the coefficient of lift used in most of the aircraft's flight time, and thickness ratio. Design lift coefficient is calculated based on cruise conditions using lift equation (Eq. ( 5)).

$$L = \frac{1}{2} \rho V^2 S C_L \quad (5)$$

We make use of the assumption that  $W=L$  during cruise. Using density of air at cruise altitude from [15], cruise speed from the requirements and wing loading from the average of the competitors we find that  $C_{L,Design} = 0.83$ .

Cruise mach number is  $M = 0.415$  [16]. At this Mach number a thickness ratio of  $t/c$ , of 15% is recommended by [1]. Reynolds number was calculated based on average chord length and stall speed of the competitors and was found to be  $11.5E6$ . Then some important characteristics of some candidate airfoils were found using Javafoil, an internet based program, and are shown below.

Airfoils	Cl_max	Cm_0	alpha_stall	Cd_min
NACA 63-815	1.78	-0.172	10	0.0056
NACA 58115	1.79	-0.065	16	0.035
NACA 0415	1.45	-0.02	15	0.00553

Table 5 Key airfoil parameters.

Among these airfoils NACA 58115 offers very good moment characteristics and the highest maximum coefficient of lift. The stall angle of attack is also higher for this airfoil. Thus NACA 58115 was chosen for this aircraft. Shape,  $C_L-C_D$ ,  $C_L$ -alpha and  $C_M$ -alpha plots of this airfoil are shown in Figure 8.

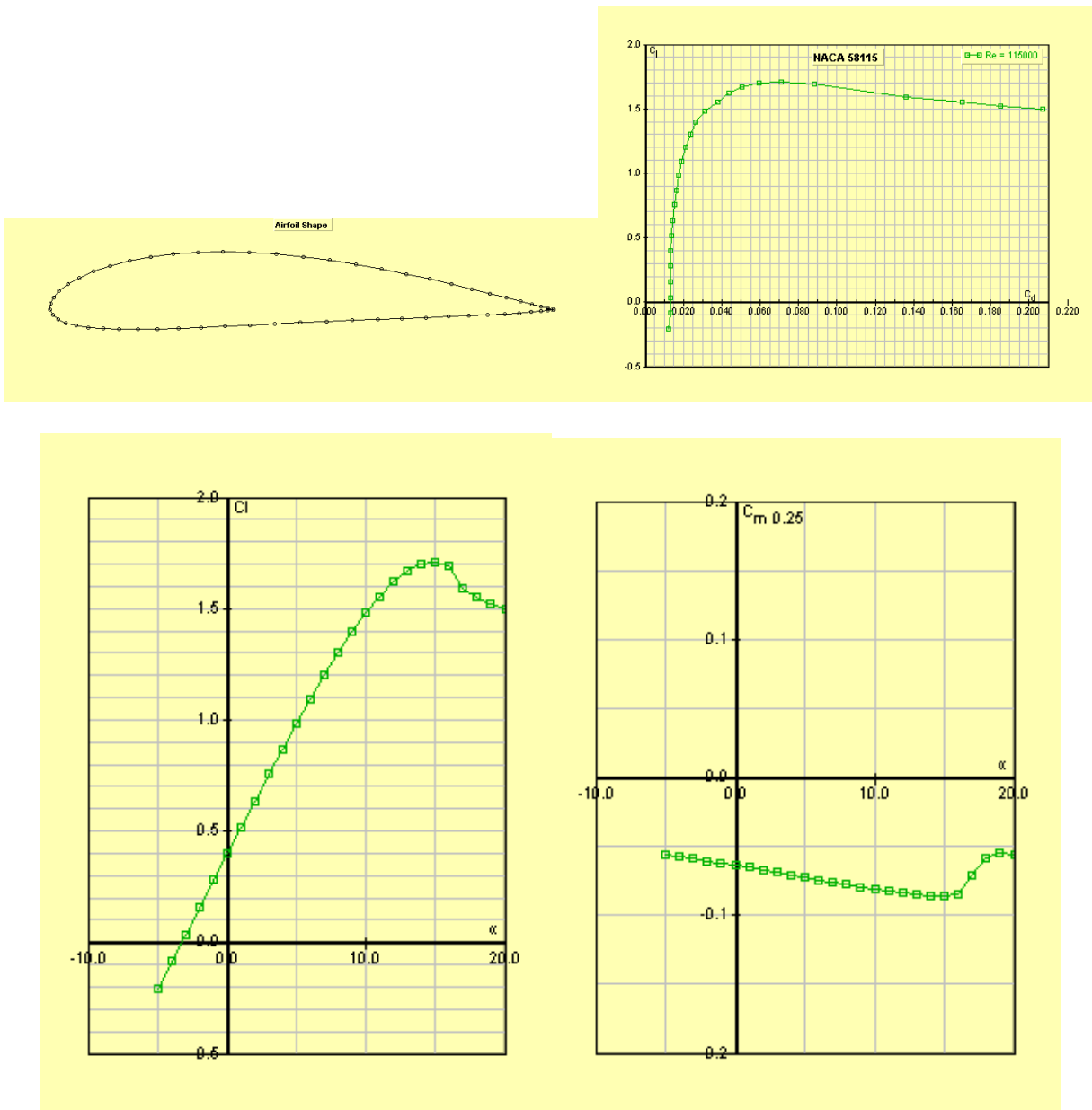


Figure 8: Shape (top left),  $C_L$ - $C_D$  plot (top right),  $C_L$ - $\alpha$  plot (bottom left) and  $C_M$ - $\alpha$  plot (bottom right) of NACA 58115.

### 4.3 OTHER WING PROPERTIES.

Figures from reference [1] suggest a maximum quarter chord sweep of  $5^\circ$  for an aircraft with an aspect ratio of 10.98 and a leading edge sweep of about  $5^\circ$  for a Mach number of 0.6 which is the maximum

Mach number for such an aircraft based on competitor data. Thus a leading edge sweep of  $2^\circ$  will be used for aesthetic reasons. This results in a quarter chord sweep of about  $1^\circ$ .

Based on historical trends provided by reference [1] a taper ratio of 0.4 is appropriate for an aircraft with a quarter chord sweep of  $1^\circ$ .

Typical twist angles range from  $0^\circ$  to  $5^\circ$  [1]. A twist of  $0^\circ$  was used in Taj Pegasus to improve manufacturability and thus decrease the cost.

# CHAPTER 5

## Design Parameters

---

“One man’s ‘magic’ is another man’s engineering. ‘Supernatural’ is a null word.”

Robert A. Heinlein

### 5.1 INTRODUCTION AND OBJECTIVES

Power to weight ratio and wing loading are perhaps two of the most important performance parameters of an aircraft. These two parameters determine how the aircraft will perform in virtually all performance related maneuvers and flight conditions. This chapter determines these two parameters using the information available so far about Taj Pegasus. Competitor aircraft information as well as various flight equations obtained from references were used throughout this chapter.

### 5.2 POWER-TO-WEIGHT RATIO

Power to weight ratio  $P/W_0$  is usually defined as the ratio of power of all the engines at maximum throttle settings at sea-level static and standard-day conditions divided by the design takeoff weight of the aircraft. Power to weight ratio  $P/W_0$  has a direct effect on the performance of an aircraft. A higher Power to weight ratio will result in higher acceleration, quicker climb, higher maximum speeds and higher turn rates. However Power to weight ratio requires for more powerful and thus larger engines. Historical data compiled by reference [1] state that a power ratio of 0.2 hp/lb is appropriate for a twin turboprop aircraft, however the average power to weight ratio of competitors shows a value of 0.117 hp/lb. There is a striking



contrast between the two. The latter value seems more appropriate since the competitor data has a very low standard deviation (about 10%) and “twin turboprop” refers to a wide variety of aircraft and it might not be appropriate for Taj Pegasus. This value of power to weight ratio cannot be used as an initial estimate, it is rather used to determine the number of engines to be used. As a rule of thumb the least number of engines exceeding this value were used. This value indicates at least 4 engines are needed which make the power to weight ratio of the aircraft equal to  $P/W = 0.16$  hp/lb.

## 5.3 THRUST AND POWER CORRECTIONS

Power level of Rolls Royce Allison T-56-A-15 Engines are given to be 4300 hp. This power level and the thrust obtained from it change when installed on the aircraft. Power offtake needed for aircraft systems needs to be subtracted from this power first. Then the drag emanating from nacelle blockage effects, cooling and other sources has to be subtracted from the thrust. Although in practice propeller efficiency has to be corrected for compressibility and scrubbing effects, these effects are to be ignored in this study as stated in the request for proposal.

### 5.3.1 Power offtake

Reference [1] provides the following statistical equation for finding the power offtake of this aircraft:

$$P_{ext} = \frac{160}{6500} * 4300 \text{ shp} = 105.8 \text{ shp} \quad (6)$$

Where 160/6500 is just a ratio of extracted power to total power obtained from statistics of airplanes. Thus a shaft power of 105.8 shp was subtracted from the total power in each engine.

### 5.3.2 Cooling Drag

Cooling the engines slows down the oncoming air and this generates a drag that has to be subtracted from the thrust of the engine at any velocity and altitude. This drag is found as shown below:

$$\left(\frac{D}{q}\right)_{cooling} = 4.9E - 7 \frac{bhp T^2}{\sigma V} \quad (7)$$

Where bhp is the brake horsepower of the engine, T is ambient temperature in Kelvins,  $\sigma$  is the ratio of density to sea level density and V is flight velocity.

### 5.3.3 Miscellaneous Drag

Miscellaneous drag is about 0.002% of the total power multiplied by dynamic pressure, as shown below [1]. This drag was reduced from the total thrust of each engine in the analyses below.

$$\left(\frac{D}{q}\right)_{misc} = 2E - 4 * bhp \quad (8)$$

## 5.4 WING LOADING

Wing loading shows how much weight each ft<sup>2</sup> of the wing reference area carries at a given flight condition. A smaller wing loading results in a larger wing. Wing loading will be calculated for each performance requirement and the largest wing loading that satisfies all the requirements will be selected at the end. This makes sure that the smallest possible wing is designed.

### 5.4.1 Cruise

The main objective in cruise is to increase range. This is done by increasing aerodynamic efficiency of the aircraft, or in other words, maximizing L/D in propeller airplanes. This happens when induced drag is equal to parasite drag. Which means we can write coefficient of lift in terms of other parameters such as Oswald span efficiency factor and parasite drag coefficient. This is shown in Eq. ( 9). Note that Eq. ( 9) is just another form of lift equation (see Eq. ( 5)) where coefficient of lift is written in terms of other parameters. Oswald span efficiency factor was calculated to be 0.731 based on aspect ratio [1], parasite drag ( $C_{D0} = 0.0267$ ) depends on skin friction coefficient and wetted area ratio. The values used for these parameters

at this stage of the design are rough values based on eyeball estimates and approximate Reynold's numbers. The graphs provided in references [1] and [13] are used for these estimations. Using this information in Eq. ( 9) we find that  $W/S = 87.66 \text{ lb/ft}^2$  is required to fulfill the cruise mission. Note that the wing loading found here was corrected for the fuel spent during takeoff and climb.

$$\frac{W}{S} = q_{\infty} \sqrt{\pi A R e C_{D0}} \quad (9)$$

### 5.4.2 Climb Rate

The requirements ask for a climb rate of 1500 ft/min at 10000 ft. altitude. Wing loading can also be estimated based on the climb rate requirements given in the requirements. The following equation is given by [1]:

$$\frac{W}{S} = \frac{\left[ \frac{T}{W} - G \right] \pm \sqrt{\left( \frac{T}{W} - G \right)^2 - 4 * k * C_{D0}}}{2k/q_{\infty}} \quad (10)$$

Where  $k = 1/(\pi A R e) = 0.0396$  and  $G = (T-D)/W = \text{Forward Speed/Upward Speed} = \text{Climb gradient}$ . Climb usually takes place at velocities higher than stall speed and lower than cruise speed for propeller airplanes. A flight speed of 250 ft/s was used for flight speed after a competitor survey. Then  $G = 0.1$ . Available power of the aircraft at 10000 ft altitude was then converted to equivalent thrust to weight ratio  $T/W$  using flight velocity and propeller efficiency. This requirement results in a wing loading of  $W/S = 361.5 \text{ lb/ft}^2$ .

### 5.4.3 Takeoff Distance

MIL-STD-3013 takeoff distance definition [17] will be used in the following calculations. This includes an obstacle clearance of 50 ft. in the takeoff distance definition. Reference [1] provides graphs for approximating the "Takeoff parameter" defined as

$$\text{Takeoff Parameter (TOP)} = \frac{W/S}{\sigma C_{L_{TO}} P/W} \quad (11)$$

Here  $\sigma$  is the ratio of air density at takeoff location divided by air density at sea level. For the purposes of this report it will be assumed that the aircraft takes off from sea level making the value of  $\sigma$  equal to 1. For a propeller aircraft with a takeoff distance of 3500 ft. takeoff parameter corresponds to roughly 450. The takeoff lift coefficient  $C_{L_{TO}}$  is hard to estimate. On the one hand performance of the airfoil will be reduced in a 3D wing which results in a smaller  $C_{L_{max}}$  for the wing than the airfoil. On the other hand high lift devices will be used which increase the lift of the airfoil. Hence the author hereby assumes that after installation of high lift devices coefficient of lift at takeoff will be equal to maximum coefficient of lift of the airfoil, thus 129.58 lb/ft<sup>2</sup>.

#### 5.4.4 Landing Distance

The request for proposal is not clear about the landing conventions but MIL-STD-3013 [17] landing field length will be used for calculation of landing distance in this part.

Reference [1] provides an equation for estimating the wing loading based on landing distance.

$$S_{\text{landing}} = 0.66 * 80 \left( \frac{W}{S} \right) \left( \frac{1}{\sigma C_{L_{max}}} \right) + S_a \quad (12)$$

Where  $C_{L_{max}}$  was found to be 1.79 for NACA 58115,  $S_{\text{landing}}$  is the landing distance and  $S_a$  is the obstacle clearance distance and it is equal to 1000 ft. for airliner type aircraft. A factor of 0.66 is included in the first term of the above expression because the aircraft has variable pitch propellers (as stated in the RFP). Then wing loading is then calculated to be  $W/S = 98.06$  lb/ft<sup>2</sup> after correcting for fuel spent during takeoff.

#### 5.4.5 Service Ceiling

Eq. (10) can also be used to calculate the wing loading necessary to attain some service ceiling. Service ceiling is defined as the altitude in which the aircraft has barely enough power to climb at 100 ft/min if

needed [1]. The request for proposal requires the aircraft to be able to fly at 33000 ft. altitude with an empty container (weight of the aircraft minus 40000 lb.). After using the appropriate weight (empty container and reduced fuel) and power at that altitude wing loading is calculated as  $W/S = 357.02 \text{ lb/ft}^2$ .

#### 5.4.6 Conclusions

Five different values were calculated for wing loading. The smallest one of these values will satisfy all the other requirements. Thus a value of  $W/S = 85.65 \text{ lb/ft}^2$  was chosen for wing loading after leaving a small margin of  $2 \text{ lb/ft}^2$ . Furthermore, it was decided that 4 engines are to be used in Taj Pegasus. Which results in a power to weight ratio of  $0.16 \text{ hp/lb}$ . It was verified that all the requirements are met with these choices of wing loading and power to weight ratio.

# CHAPTER 6

## Refined Sizing

“I have not failed, but found 1000 ways to not make a lightbulb.”

Thomas Edison

### 6.1 EMPTY WEIGHT FRACTION

Empty weight fraction can be estimated based on advanced statistical equations. One such equation is given in reference [1] and reported below:

$$\frac{W_e}{W_0} = a + bW_0^{C1}AR^{C2} \left(\frac{P}{W_0}\right)^{C3} \left(\frac{W_0}{S}\right)^{C4} V_{max}^{C5} \quad (13)$$

This weight estimate is more accurate because it accounts for many different factors when giving a weight estimate such as initial takeoff weight estimate, aspect ratio, power to weight ratio, wing loading and maximum speed. All of these variables with the exception of maximum speed are already calculated. Maximum speed  $V_{max} = 420.1$  was found from the average of the competitors. Values of the constants in Eq. (13) for a twin turboprop aircraft are given as shown below:

Type	a	b	C1	C2	C3	C4	C5
Twin Turboprop	0.37	0.08	-0.06	0.08	0.08	-0.05	0.3

Table 6: List of parameters used in the statistical sizing equation.

Eq.(13) is a very useful equation even for learning how various factors affect aircraft weight. For example Eq. (13) implies that increasing aspect ratio will result in a heavier airplane. This makes sense because longer wings will generate larger moments at the root. Hence stronger and heavier materials are used at the root to strengthen the wings. Fuel weight fraction of the aircraft was calculated to be  $W_f/W_0 = 0.172$  based on the same method as section 0 but using updated input data.

Then weight of Taj Pegasus is calculated iteratively to be  $W_0 = 16964.1$  lb. assuming composites structures are widely used in the aircraft. Similarly empty weight and fuel weight of the aircraft are 75927.8 lb. and 25296.3 lb. respectively.

# CHAPTER 7

## Geometry, Sizing and Configuration

---

“If it looks good it will fly good.”

Bill Lear

### 7.1 FUEL VOLUME

A fuel weight of 25296.3 lb. was calculated previously. Assuming this aircraft uses JP-8/JETA1 fuel we calculate the volume of the carried fuel to be

$$V = \frac{22078.0}{6.7} = 3775.6 \text{ gal} = 504.8 \text{ ft}^3 \quad (14)$$

Where 6.7 lb/gal is the density of JP-8/JETA1 from [1]. There are three locations on the aircraft used for fuel storage. These are the fuselage, the wings and external canopies. Among these three options the wings provide the most useful alternative as shown below:

- Fuel is close to the center of gravity, which makes the aircraft easily controllable at all times.
- The risk of catching fire is diminished. (As opposed to storing the fuel in the fuselage)
- In case of fire the passengers, crew and payload are relatively safe. (As opposed to storing the fuel in the fuselage)
- No additional drag. (As opposed to external fuel tanks)

Thus the fuel will be stored in wing integral tanks.



85% of the volume measured external surface is usable for wing integral tanks [1]. Also 3-5% volume will be allocated for fuel expansion in warm weather. Then  $V_f = 440.5/0.85/0.95 = 625.14 \text{ ft}^3$

## 7.2 WING SIZING AND PLANFORM SHAPE

Wing area is calculated from weight and wing loading as  $S = W_0/(W_0/S) = 1715.7 \text{ ft}^2$ . Then the following geometric characteristics are calculated for the wing using aspect ratio and taper ratio found previously:

Span	Root Chord ( $C_r$ )	Tip Chord ( $C_t$ )	MAC	$y_{MAC}$
137.38	17.8	7.1	13.3	29.4

Table 7: Wing Geometric characteristics. All units are in ft. (Note: MAC stands for Mean Aerodynamic Chord and  $y_{MAC}$  is the spanwise location of MAC)

Also note that a high wing configuration was used to allow room for the container at the bottom and a dihedral angle of -3 degrees was given to the wings to avoid an overly stiff airplane. The keywords used in this section are shown graphically in Figure 9.

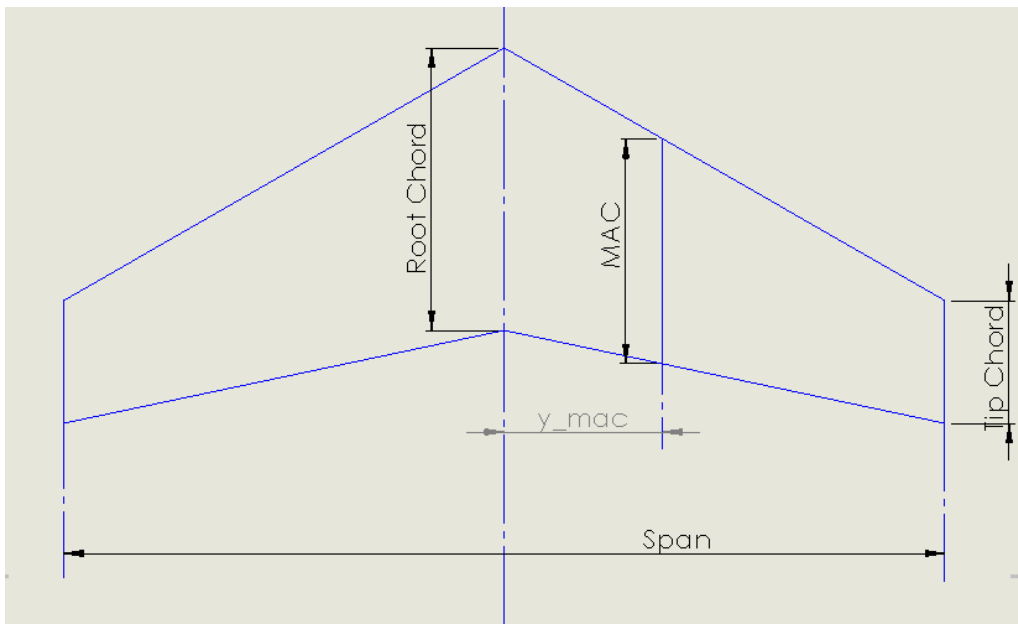


Figure 9: Figure showing wing terminology graphically.

### 7.3 FUSELAGE LENGTH

Historical trends shown in reference [1] result in a fuselage length of 83.9 ft for this aircraft. Average fuselage length of the competitors was previously found to be 102.5 ft. The aircraft designed in this report does not need a very long fuselage. The payload this aircraft will carry has a length of 20 ft which can easily fit in the airplane even if the fuselage is short. Thus a length of  $l_f = 80$  ft will be used.

### 7.4 TAIL SIZING AND PLANFORM SHAPE

There are many different alternatives for tail configuration that could be used in this aircraft. Some tail configurations used in airplanes in the past are shown in the figure below:

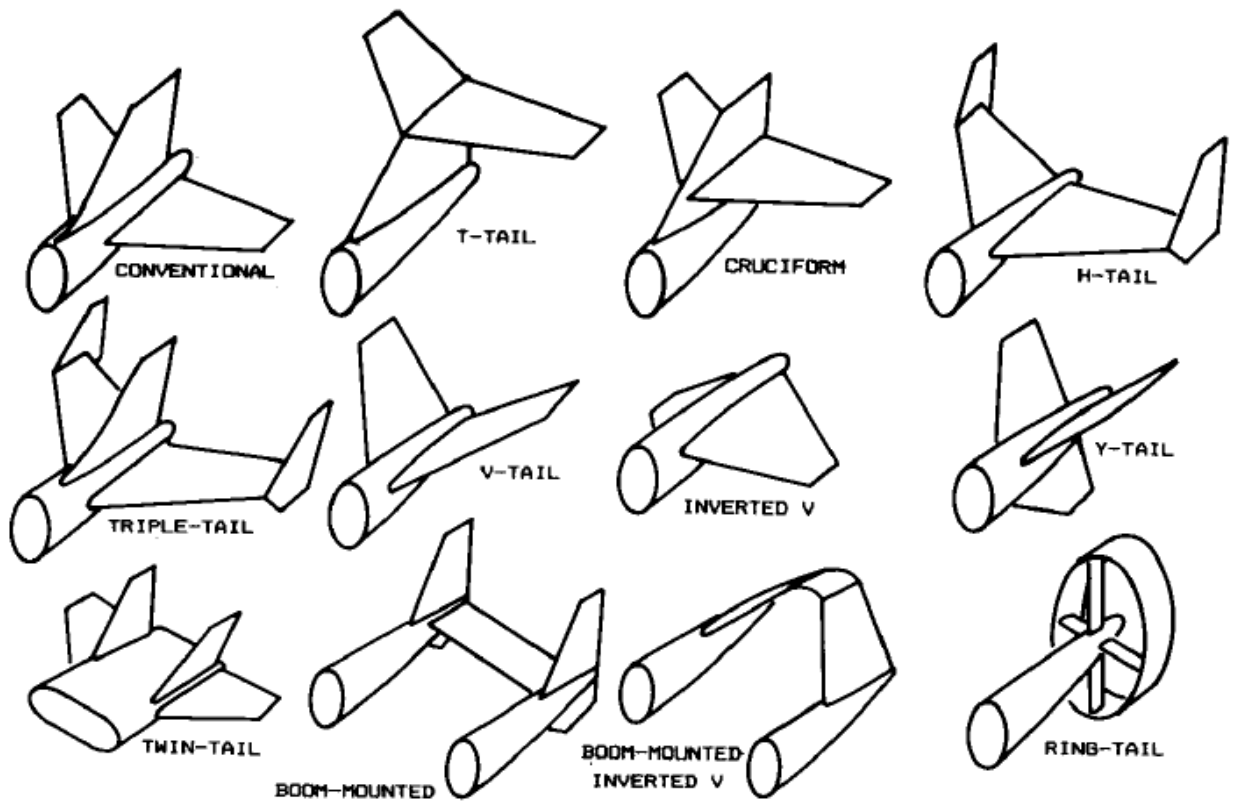


Figure 10: Tail configurations. Figure obtained from [1].

Among the alternatives conventional tail is the most used tail configuration. However other configurations are also used from time to time based on the specific needs of the aircraft being designed. For Taj Pegasus, other than conventional tail boom mounted tail also looks promising due to the ease in loading and unloading that this tail could provide. The following table summarizes the advantages and disadvantages of the two tail configurations.

Configuration	Advantages	Disadvantages
<b>Conventional</b>	<ul style="list-style-type: none"> <li>• Lighter tail</li> <li>• Easier production (low cost)</li> <li>• Since the rear of the fuselage is already extending well beyond wing trailing edge, tail arm will be small and thus lightweight.</li> </ul>	<ul style="list-style-type: none"> <li>• Could hinder loading and unloading of the container.</li> </ul>
<b>Boom Mounted</b>	<ul style="list-style-type: none"> <li>• Horizontal tail is more effective because the vertical tails act as winglets.</li> <li>• Vertical tails could be made more effective by placing them in the propwash.</li> </ul>	<ul style="list-style-type: none"> <li>• Heavier tail</li> <li>• Heavier arm</li> <li>• Higher cost</li> <li>• Higher drag</li> </ul>

*Table 8: Candidate tail configurations for TAJ PEGASUS.*

After considering the advantages and disadvantages of each, conventional tail was chosen to be used in Taj Pegasus.

### 7.4.1 Tails

The tails were sized with methods outlined in [1]. Vertical tail was placed slightly ahead of horizontal tail to avoid horizontal tail wake on the vertical tail in high angles of attack. The following table summarizes tail properties.

Tail	S (ft <sup>2</sup> )	AR	$\lambda$	l (ft)	Span (ft)	Root Chord (C <sub>r</sub> ) (ft)	Tip Chord (C <sub>t</sub> ) (ft)	MAC (ft)	y <sub>MAC</sub> (ft)
Horizontal	473.7	3.0	0.4	48	37.7	18.0	7.2	13.3	8.1
Vertical	392.8	2.0	0.4	48	28.0	20.0	8.0	14.9	6.0

Table 9: Tail geometric characteristics. (Note: MAC stands for mean aerodynamic chord and y<sub>MAC</sub> is the spanwise location of MAC. l is the distance from wing MAC to tail MAC.)

## 7.5 ENGINE AND PROPELLER DIMENSIONS AND WEIGHT

As stated previously 4 Rolls Royce Allison T-56-A-15 Engines will be used. The following properties were found for this engine:

Type	Weight (uninstalled) (lb.)	Length (ft.)	Diameter (ft.)	SFC (dry) (lbs/hp/hr)	Power (SLS) (SHP)	Propeller	Propeller Diameter (ft)
Turboprop	1940	12.17	2.25	0.5	4300	NP2000	13.5

Table 10: Engine characteristics.

# CHAPTER 8

## Preliminary CG Estimation, Landing Gear Placement and Sizing

---

“Only from the heart can you touch the sky.”

Rumi

### 8.1 WEIGHTS OF MAJOR COMPONENTS

At this point a simple 3D model of the airplane was drawn in OpenVSP, a computer aided design software made specifically for airplane design. This drawing is shown below.

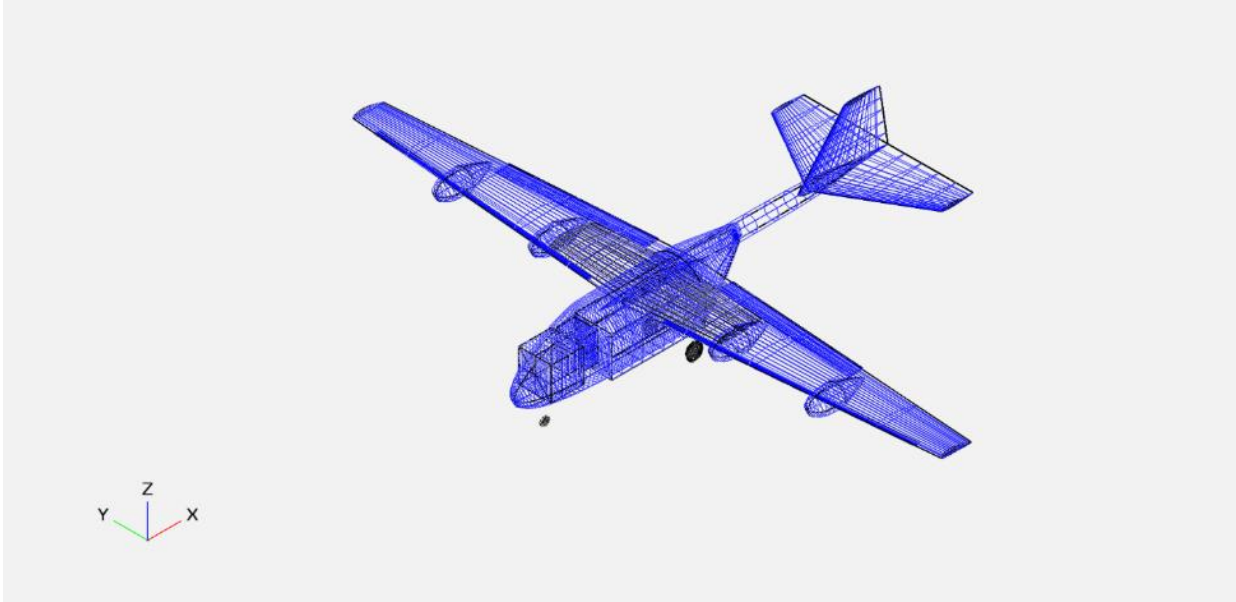


Figure 11: A CAD drawing of Taj Pegasus prepared in OpenVSP.

This drawing was used to obtain the reference parameters for the following parts.

Weights of major components of the aircraft can be calculated using tables given in [1]. These weights and parameters used as bases for calculating these weights are shown in the table below.

Component	Wing	Horizontal Tail	Vertical Tail	Fuselage
Reference Parameter	Exposed Area	Exposed Area	Exposed Area	Wetted Area
Weight (lb.)	13725.6	2423.1	2160.6	7060

Landing Gear	All-Else	Fuel	Engines	Container	Takeoff Design Weight
Takeoff Design Weight	Takeoff Design Weight	-	-	-	-
5818.6	23003.7	23291.4	10088.0	45140.0	<b>135316</b>

Table 11: Takeoff Design Weight calculation based on component weights.

Note that weight of fuel, engines and container are either available from the RFP or calculated in previous parts. Takeoff design weight was calculated by summing all the component weights and landing gear and all-else weight were calculated iteratively based on takeoff design weight.

## 8.2 LANDING GEAR PLACEMENT AND SIZING

Landing gear placement is one of the trickiest part of airplane design. It most often results in a complete revision of the design. This is especially the case for the aircraft designed in this report. The author opted for swift loading and unloading of the container and the container has to be carried externally. This makes landing gear placement complicated. Since Lockheed Martin C130J Hercules is similar to this aircraft in many senses its landing gear was used as a reference. A tricycle (conventional) landing gear was used however wheel base (distance between nose and main landing gears) was reduced considerably because this aircraft is much shorter. Then landing gears were placed such that most of the weight (>80%) is carried by the main landing gear, as is the case with most aircraft [1].

Center of gravity of the aircraft is located 26 ft. aft and 3.5 ft. above the nose. Landing gear positions are shown in the figure below.

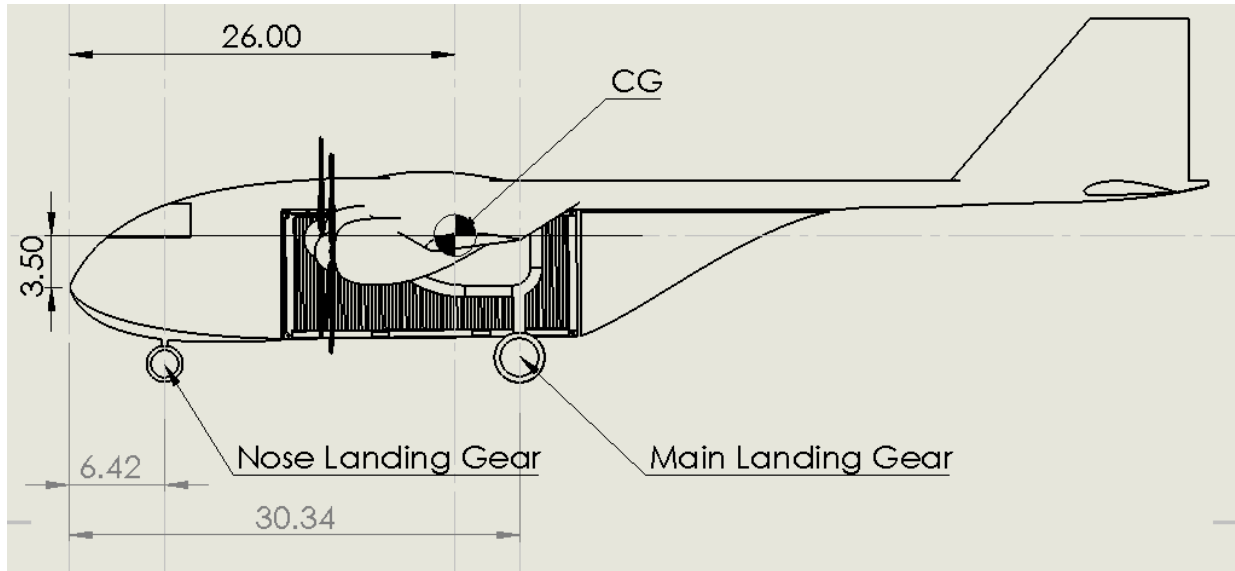


Figure 12: Position of CG and landing gears. All dimensions are in ft.

With a simple geometrical calculation using these distances it was determined that nose and main landing gears carry 19102.0 lb. (18.2%) and 105712.4 lb. (81.8%) respectively.

As mentioned before landing gears and tires are modelled after Lockheed Martin C130J Hercules. C130J has two tires in the front landing gear in parallel and two in each main landing gear in tandem. This exact configuration will also be used here. Diameters and widths of the tires are calculated based on historical trends given in [1].

	Diameter (ft.)	Width (ft.)
<b>Nose Landing Gear</b>	2.43	0.71
<b>Main Landing Gear</b>	3.36	1.15

Table 12: Landing gear tire dimensions.

Later some critical angles in landing gear design such as tipback and taildown angle and the angle that the CG makes with main landing gear are calculated and shown in the table and figures below. Tipback angle is the angle that main landing gear makes with the rearmost part of the aircraft. Taildown angle is the



same as tipback angle except this angle is measured when the landing gear strut is contracted. The minimum limits for these angles are taken from [14]. These angles are also shown in Figure 13.

	Tipback Angle	Taildown Angle	CG Angle
Value (deg.)	17.89	16.07	29.71
Minimum Allowed Limit (deg.)	-	15	Tipback Angle or 15 deg

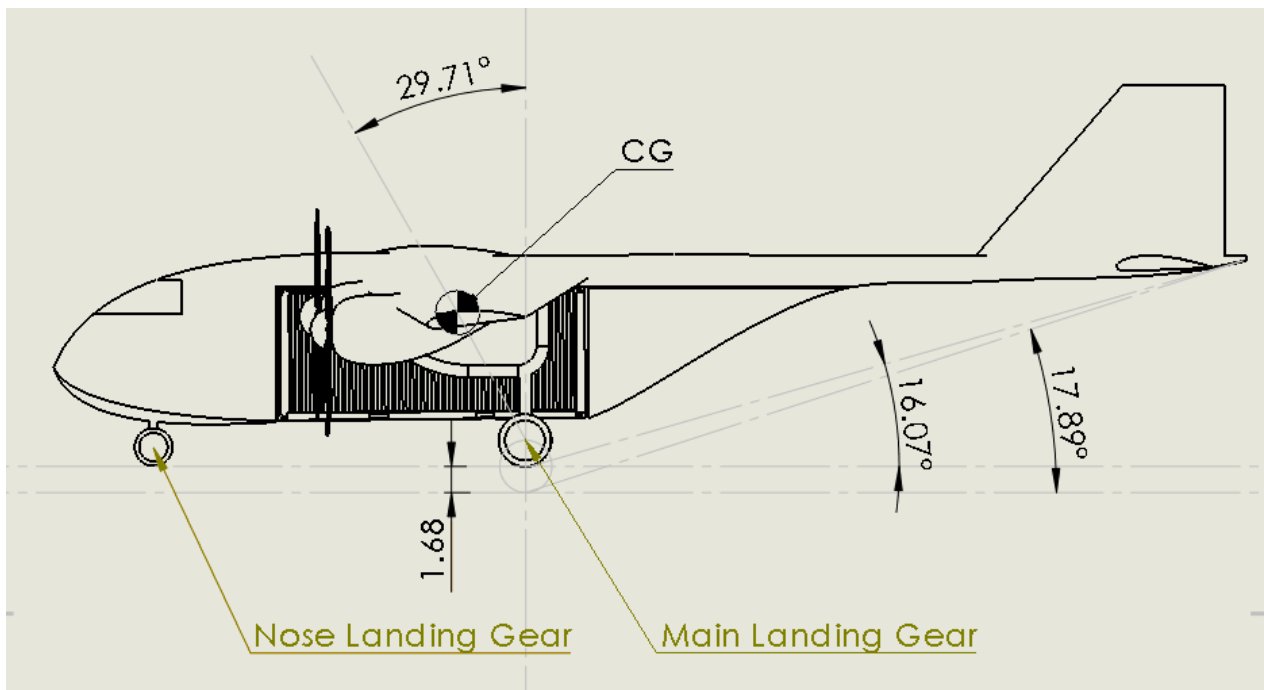


Figure 13: Tipback, taildown and CG angles of Taj Pegasus.

# CHAPTER 9

## Aerodynamics

---

“When I meet God, I am going to ask him two questions: Why relativity? And why turbulence? I really believe he will have an answer for the first.”

Werner Heisenberg

### 9.1 LIFT CURVE SLOPE

When plotting lift curve of an aircraft two parameters are needed; slope of the lift curve and its maximum value. For a subsonic aircraft the slope of the lift curve is affected by various parameters such as fuselage lift factor, exposed wing area, reference wing area, aspect ratio, wing sweep, compressibility factor and airfoil efficiency. Definitions of these parameters and the formula used for calculation of lift curve is shown in detail in reference [1]. The lift curve was found to be  $C_{L\alpha} = 5.5$  at aircraft design conditions.

Maximum lift coefficient of an aircraft is considerably different than that of the airfoil even in clean configuration (no high lift devices). Thus maximum lift coefficient had to be corrected for higher Mach numbers and 3D effects. The resulting maximum coefficient of lift and lift curves are shown in the figures below. Maximum lift coefficient was also calculated with high lift devices . A slotted flap and a leading edge flap were used for high lift devices.

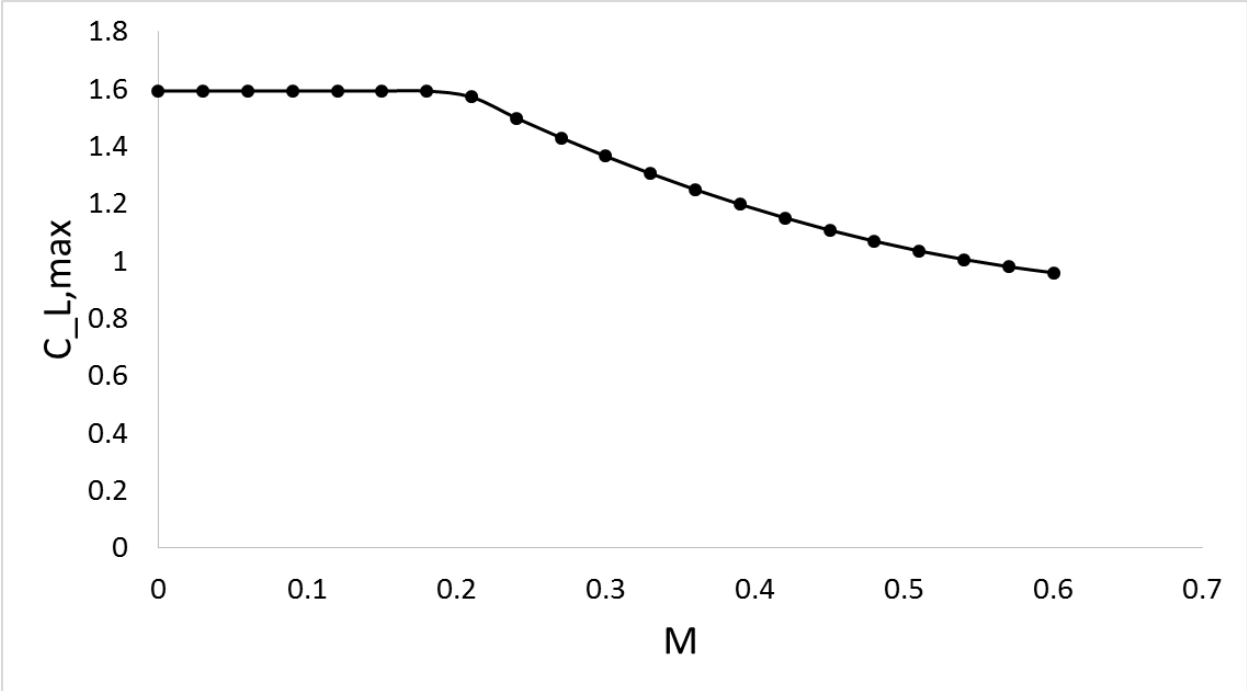


Figure 14: maximum coefficient of lift versus Mach number in clean configuration.

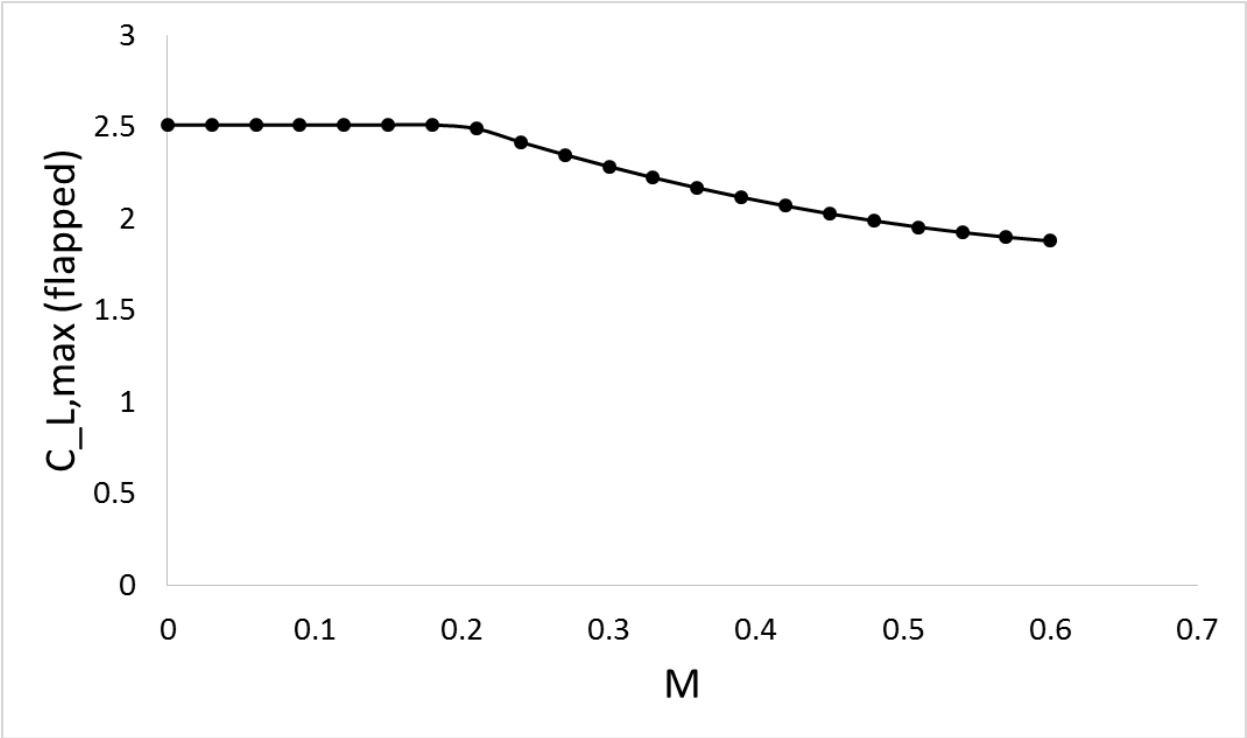


Figure 15: Maximum coefficient of lift versus Mach number with high lift devices.

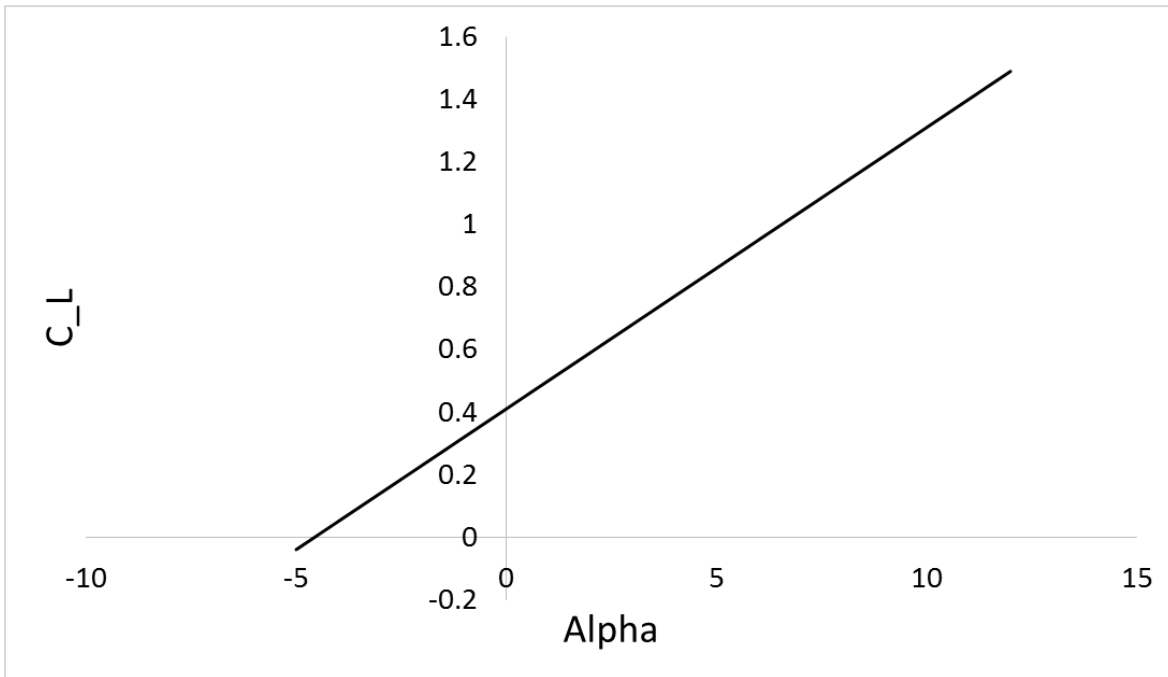
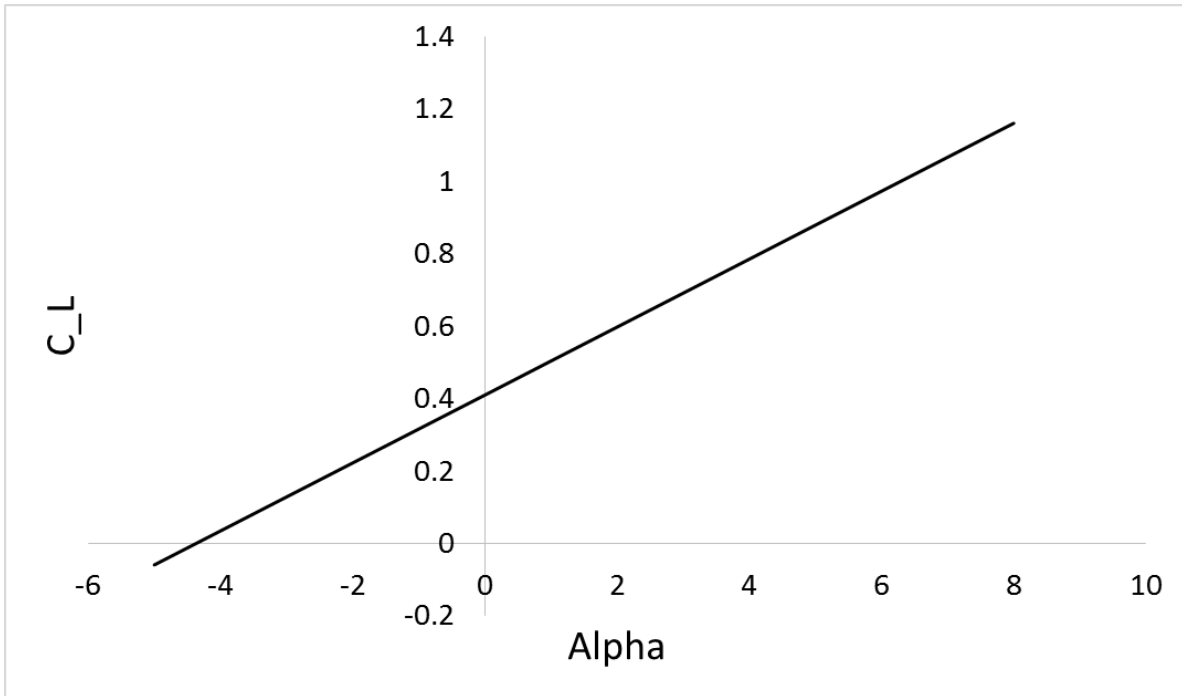


Figure 16: Coefficient of lift versus angle of attack at cruise velocity (Top) and climb velocity (Bottom).

## 9.2 DRAG

Drag of the aircraft is composed of two parts; parasite drag and induced drag. Parasite drag is calculated using the component buildup method, in which contribution of each component to drag is calculated separately and then added together. The drag of all components with the exception of the container are calculated using the methods outlined in [1] and assuming the most turbulent winds. The surface of the container is corrugated and as such the methods used for other parts are not sufficient for it. As such the methods of [18] were used instead. The parasite drag coefficient depends on skin friction coefficient, form factor, interference factor and etc. Component buildup method is explained in detail in references [1], [13]. Induced drag or so called “drag due to lift” depends largely on the aspect ratio of the wings and Oswald span efficiency factor. As the name suggests induced drag coefficient changes with lift coefficient. When all this is put together a drag polar is obtained for the aircraft which is shown in Figure 17.

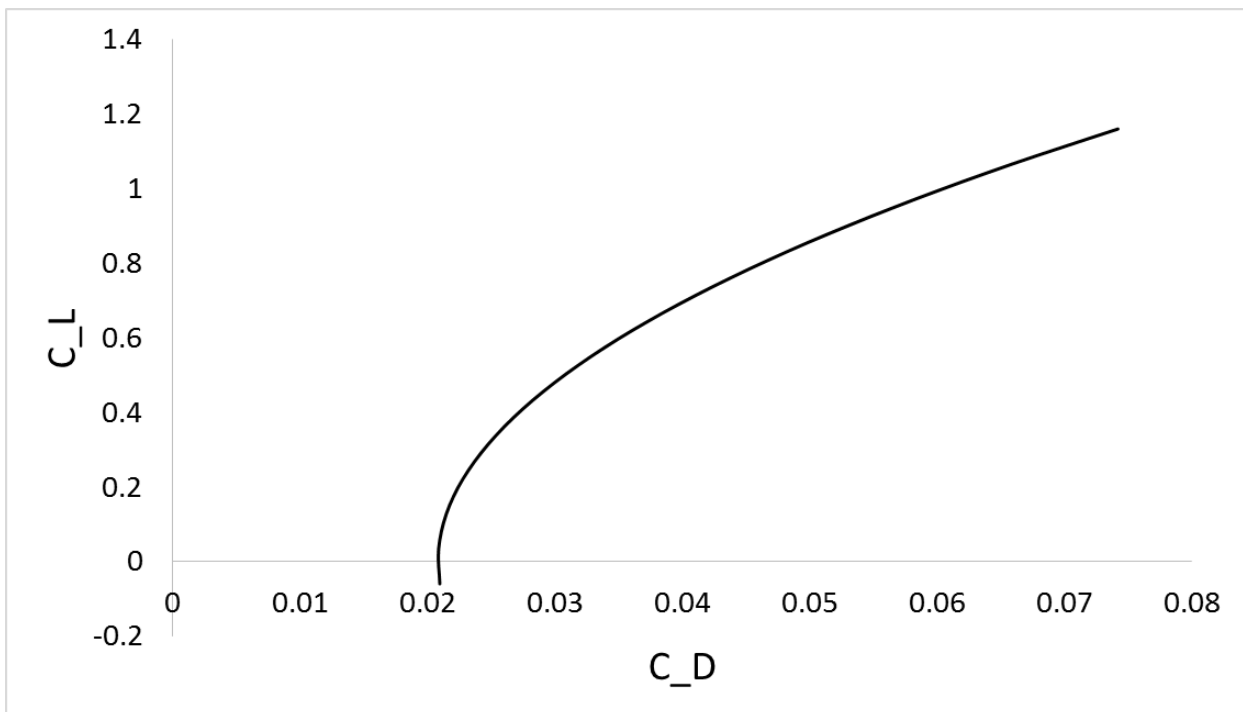


Figure 17: Drag polar of TAJ PEGASUS at its design conditions.

# CHAPTER 10

## Performance

---

“You were born with wings, why prefer to crawl through life?”

Rumi

### 10.1 POWER CURVES

Available power is fairly constant with velocity. However power required varies with velocity at a given altitude. The figure below shows these changes graphically.

There are some important points on this graph that have serious implications for the performance of the aircraft. The point where power available and power required curves meet shows the maximum velocity that the aircraft can reach at that altitude and weight. The point on the power available curve that is tangent to a straight line drawn from the origin shows the velocity at which range is maximized. In other words, it is the cruise velocity of the aircraft. The left end of power required curve shows the stall speed at these conditions. The point where power required and power available curves are furthest apart from each other shows the velocity at which maximum rate of climb is reached at that altitude. These velocities are summarized in the table below.

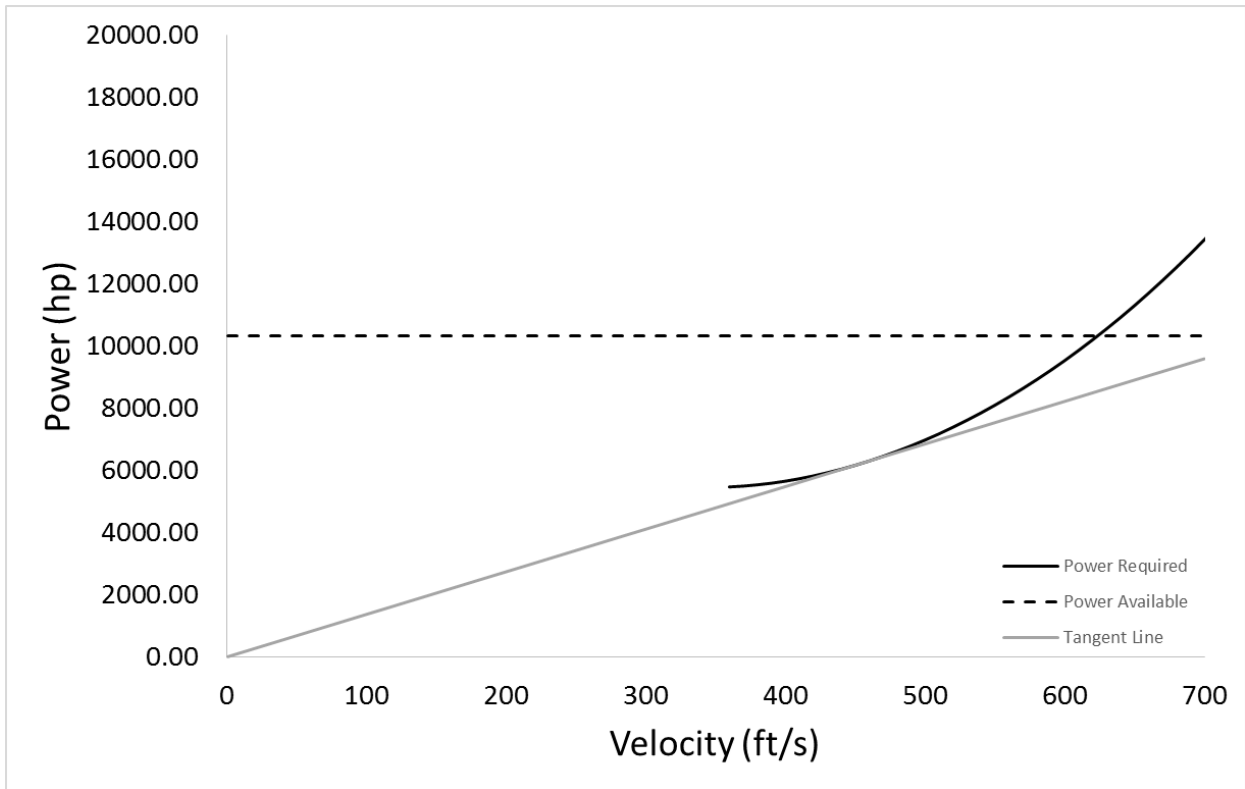


Figure 18: Power curve of TAJ PEGASUS at 23000 ft altitude and 131250.2 lb weight.

Quantity	Cruise Velocity (ft/s)	Maximum Velocity (ft/s)	Stall Velocity (ft/s)
Value	450	610	360

Table 19: Some important velocity values of TAJ PEGASUS at 23000 ft. altitude and 124814.4 lb. weight.

Note that the cruise velocity of 450 ft/s or 266.6 knot exceeds the required minimum cruise velocity of 250 knot.

At this velocity the aircraft has a lift to drag ratio of 17.2 which results in a range of 1192 nmi. when used in Breguet range equation [1]. This also exceeds the range requirement of 1000 nm.

Another power curve is shown in Figure 20 for an altitude of 10000 ft. to evaluate the climb rate requirement. From this graph it can be seen that the velocity for maximum rate of climb at 10000 ft is 310 ft/s which corresponds to a climb rate of 2512.0 ft/min. This is greater than the required climb rate of 1500 ft/min.

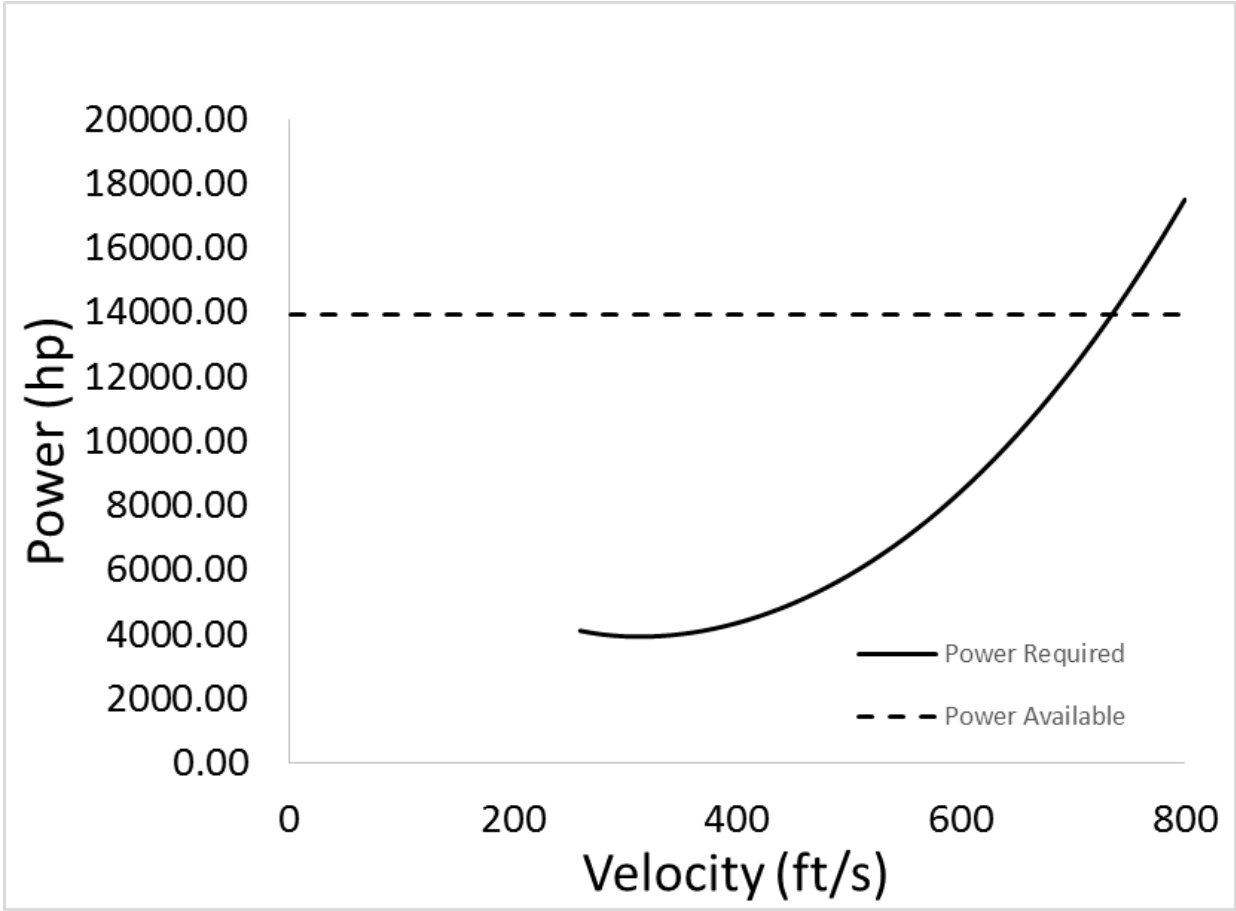


Figure 20: Power Curve of TAJ PEGASUS at 10000 ft. altitude and 131250.2 lb. weight.

The same method as Section 5.4.5 can be used to find the service ceiling. Service ceiling is the altitude at which the aircraft has just enough power to climb at 100 ft/min or 1.67 ft/s. Note that the service ceiling requirement has to be met with empty container. Using the climb rate equation of Section 5.4 Service ceiling was then found to be 47500 ft. This exceeds the required service ceiling of 33000 ft. The power curve at this altitude is shown in Figure 21.



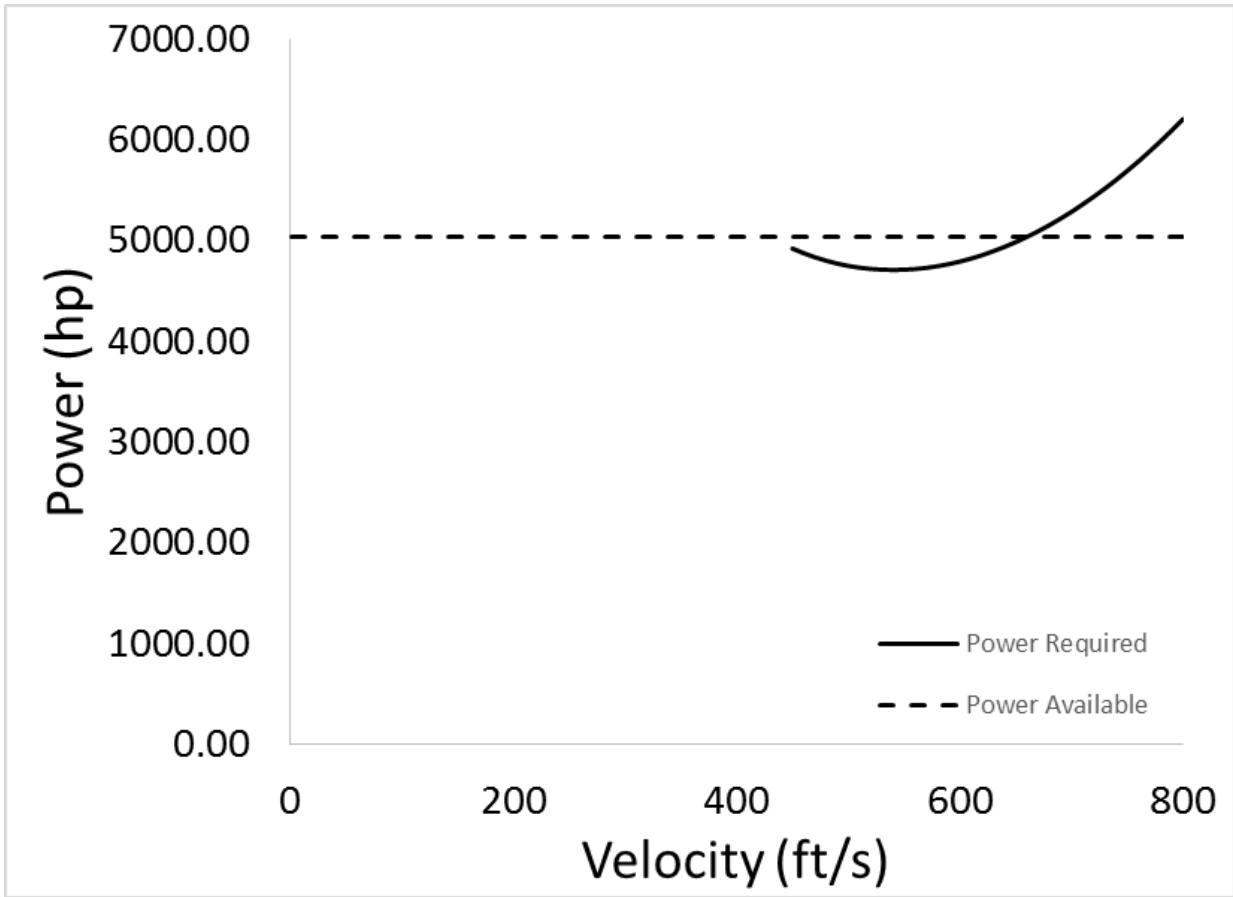


Figure 21: Power Curve of Taj Pegasus at 47500 ft. altitude and 91250.2 lb weight.

## 10.2 TAKEOFF AND LANDING DISTANCES

Using the maximum  $C_L$  value calculated in the previous chapter and the most recent values for wing loading and power to weight ratio takeoff distance was calculated to be 2800 ft based on the methods of section 5.4.3. This is less than the required maximum takeoff distance of 3500 ft.

Similarly landing distance was found to be 2801.5 ft using the same method as section 5.4.4.

# CHAPTER 11

## Optimization Matrix and Carpet Plots

---

“It is possible to fly without motors, but not without knowledge and skill.”

Wilbur Wright

The aircraft designed so far in this report fulfills all the requirements. However the question of whether this is the lightest design that does so remains. To answer this question an optimization was performed on the aircraft. First eight new combinations of power and wing loading were used to design the airplane. For the optimization process to be effective some of the designs should fail. So moderately different values were selected for these parameters. The power levels chosen correspond to 3, 4 and 5 engines respectively and wing loading values are 80%, 100% and 120% of the baseline design. A summary of these designs is given in the figure below.

	$W_0/S = 68.6 \text{ lb/ft}^2$	$W_0/S = 85.7 \text{ lb/ft}^2$	$W_0/S = 102.8 \text{ lb/ft}^2$
P = 12900 bhp	<b>#1</b> <b><math>W_0 = 136057.8 \text{ lb.}</math></b> Cruise Speed: 242.9 kts. Range: 1128.6 nmi. R/C: 1648.44 ft./min Service Ceil.: 43200 ft. TO Dist.: 3400 ft. Land. Dist.: 2500.7 ft.	<b>#2</b> <b><math>W_0 = 126569.5 \text{ lb.}</math></b> Cruise Speed: 266.7 kts. Range: 1192.0 nmi. R/C: 1734.1 ft./min Service Ceil.: 43600 ft. TO Dist.: 3900 ft. Land. Dist.: 2688.3 ft.	<b>#3</b> <b><math>W_0 = 121973.8 \text{ lb.}</math></b> Cruise Speed: 296.2 kts. Range: 1286.2 nmi. R/C: 2706.0 ft./min Service Ceil.: 43100 ft. TO Dist.: 4000 ft. Land. Dist.: 2842.3 ft.
	<b>#4</b> <b><math>W_0 = 141006.6 \text{ lb.}</math></b> Cruise Speed: 242.9 kts. Range: 1128.6 nmi. R/C: 2373.7 ft./min Service Ceil.: 47300 ft. TO Dist.: 2700 ft. Land. Dist.: 2525.6 ft.	<b>#5 Baseline Design</b> <b><math>W_0 = 131250.2 \text{ lb.}</math></b> Cruise Speed: 266.7 kts. Range: 1193.0 nmi. R/C: 2512.0 ft./min Service Ceil.: 47500 ft. TO Dist.: 2800 ft. Land. Dist.: 2712.6 ft.	<b>#6</b> <b><math>W_0 = 126493.3 \text{ lb.}</math></b> Cruise Speed: 296.2 kts. Range: 1286.2 nmi. R/C: 3512.6 ft./min Service Ceil.: 47100 ft. TO Dist.: 2950 ft. Land. Dist.: 2873.0 ft.
	<b>#7</b> <b><math>W_0 = 145874.4 \text{ lb.}</math></b> Cruise Speed: 242.9 kts. Range: 1128.6 nmi. R/C: 3052.0 ft./min Service Ceil.: 50300 ft. TO Dist.: 2200 ft. Land. Dist. 2542.5 ft.	<b>#8</b> <b><math>W_0 = 135835.6 \text{ lb.}</math></b> Cruise Speed: 266.6 kts. Range: 1192.9 nmi. R/C: 3238.7 ft./min Service Ceil.: 50500 ft. TO Dist.: 2300 ft. Land. Dist. 2736.3 ft.	<b>#9</b> <b><math>W_0 = 130957.2 \text{ lb.}</math></b> Cruise Speed: 296.2 kts. Range: 1286.2 nmi. R/C: 4265.5 ft./min Service Ceil.: 50100 ft. TO Dist.: 2400 ft. Land. Dist. 2902.2 ft.

Table 13: 9 different combinations of power and wing loading and the resulting airplanes.

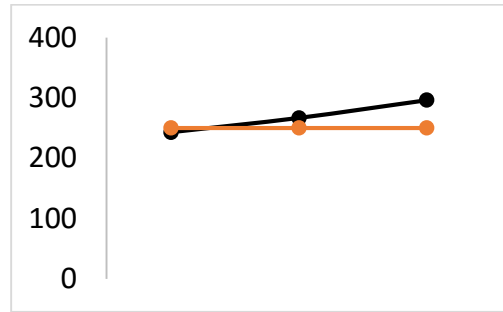
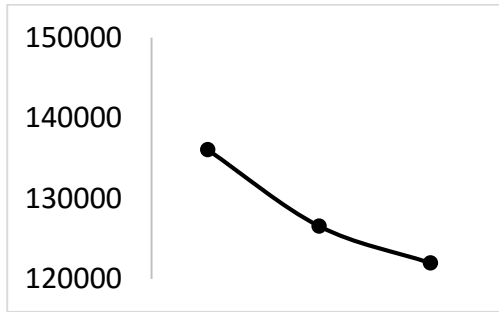
Then all the variables shown above including the weight were plotted against wing loading for every power level.

W<sub>0</sub> (lb.)

Cruise speed (kts.)

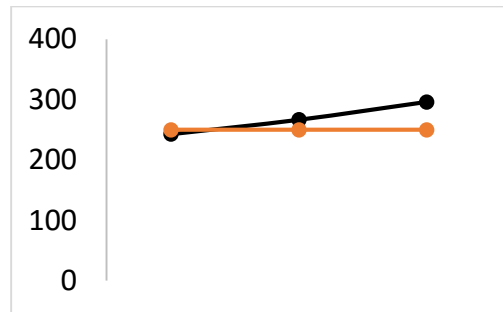
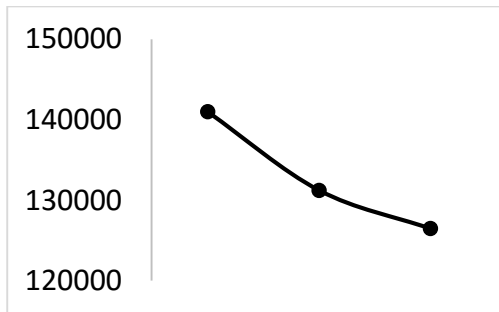
P = 12900

bhp



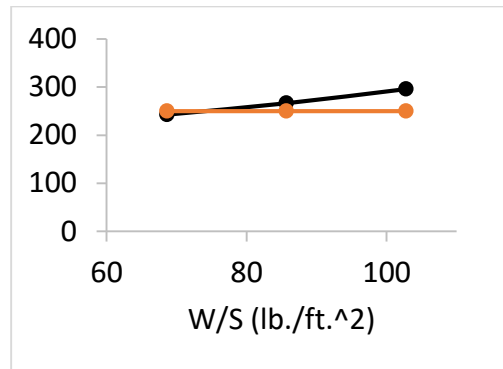
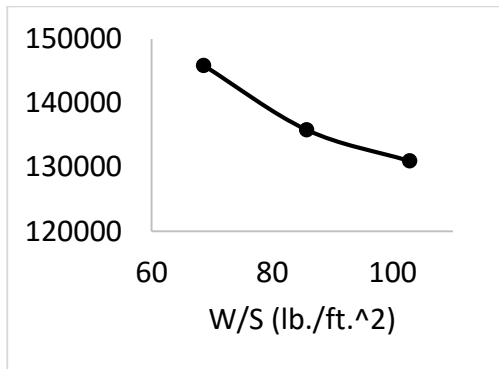
P = 17200

bhp



P = 21500

bhp

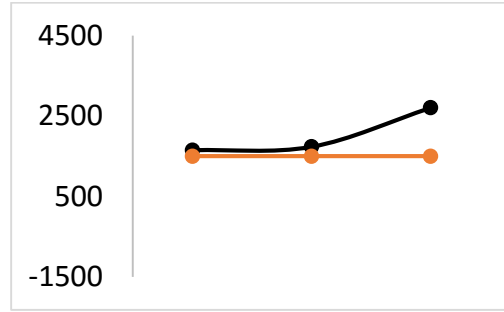
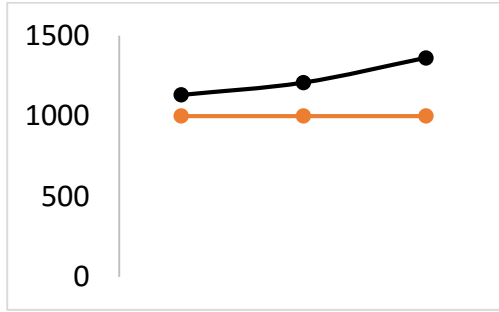


Range (nmi.)

R/C (ft/min)

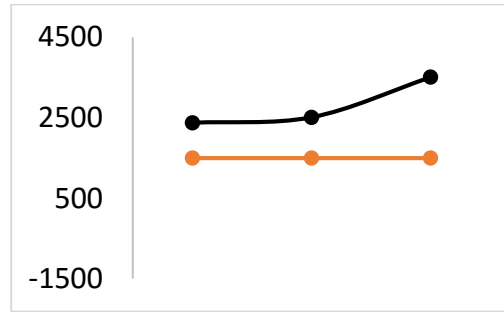
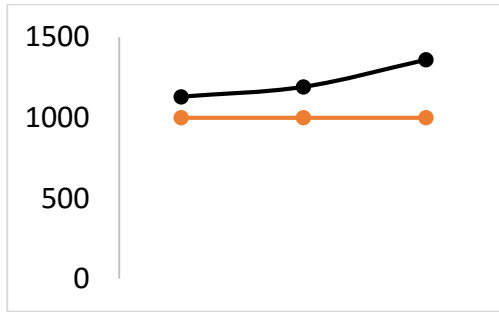
P = 12900

bhp



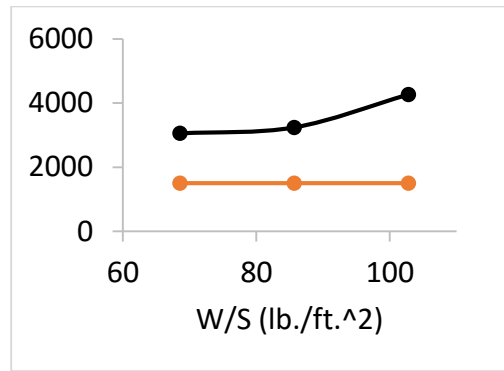
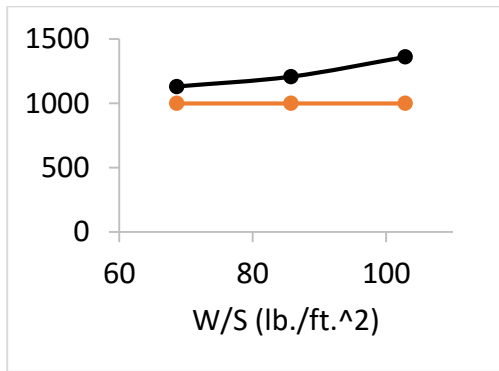
P = 17200

bhp



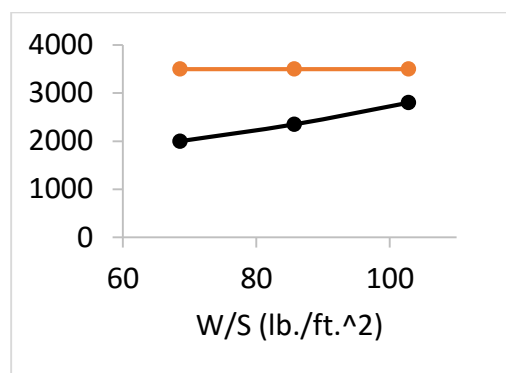
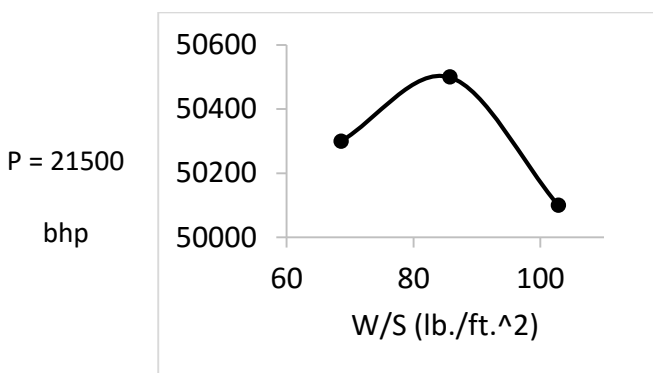
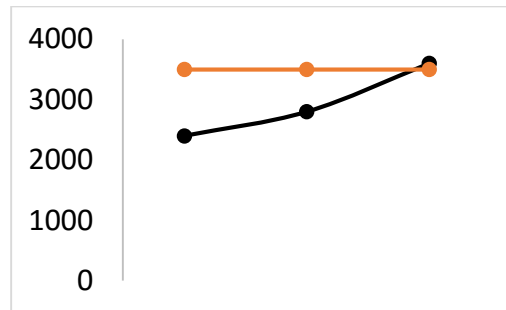
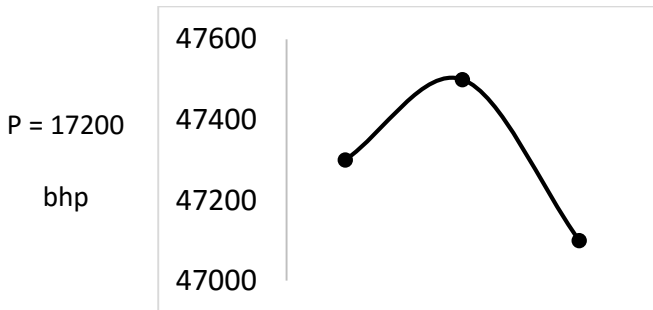
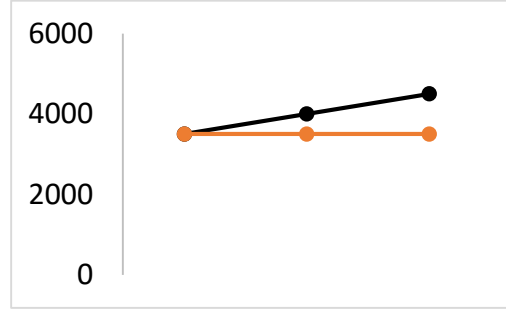
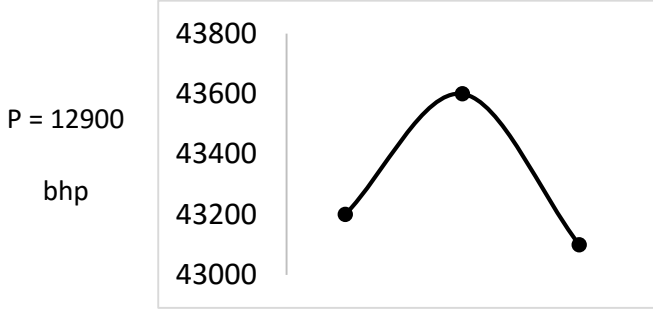
P = 21500

bhp

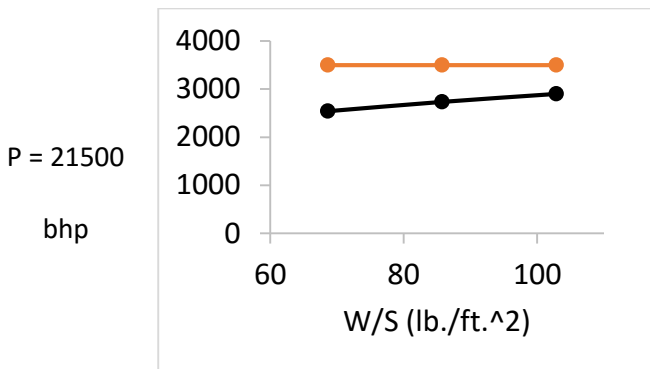
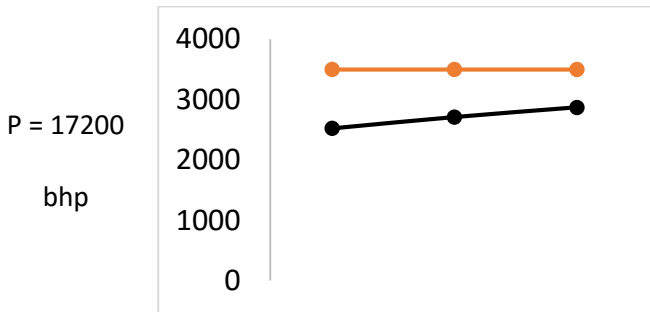
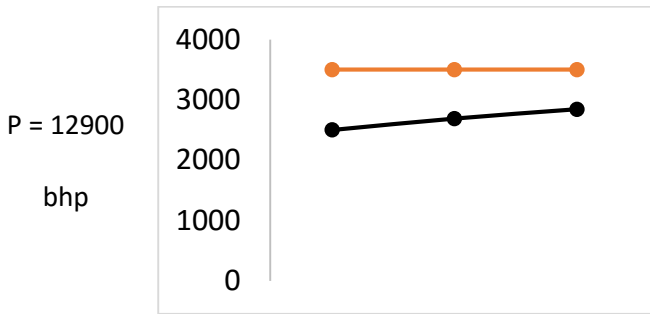


Service Ceiling (ft.)

Takeoff Distance (ft.)



Landing Distance (ft.)



Note that the orange lines show the requirements set forth by the request for proposal. Then the results were cross plotted in a power vs. wing loading plot. This plot is used to find the best point to design the airplane.

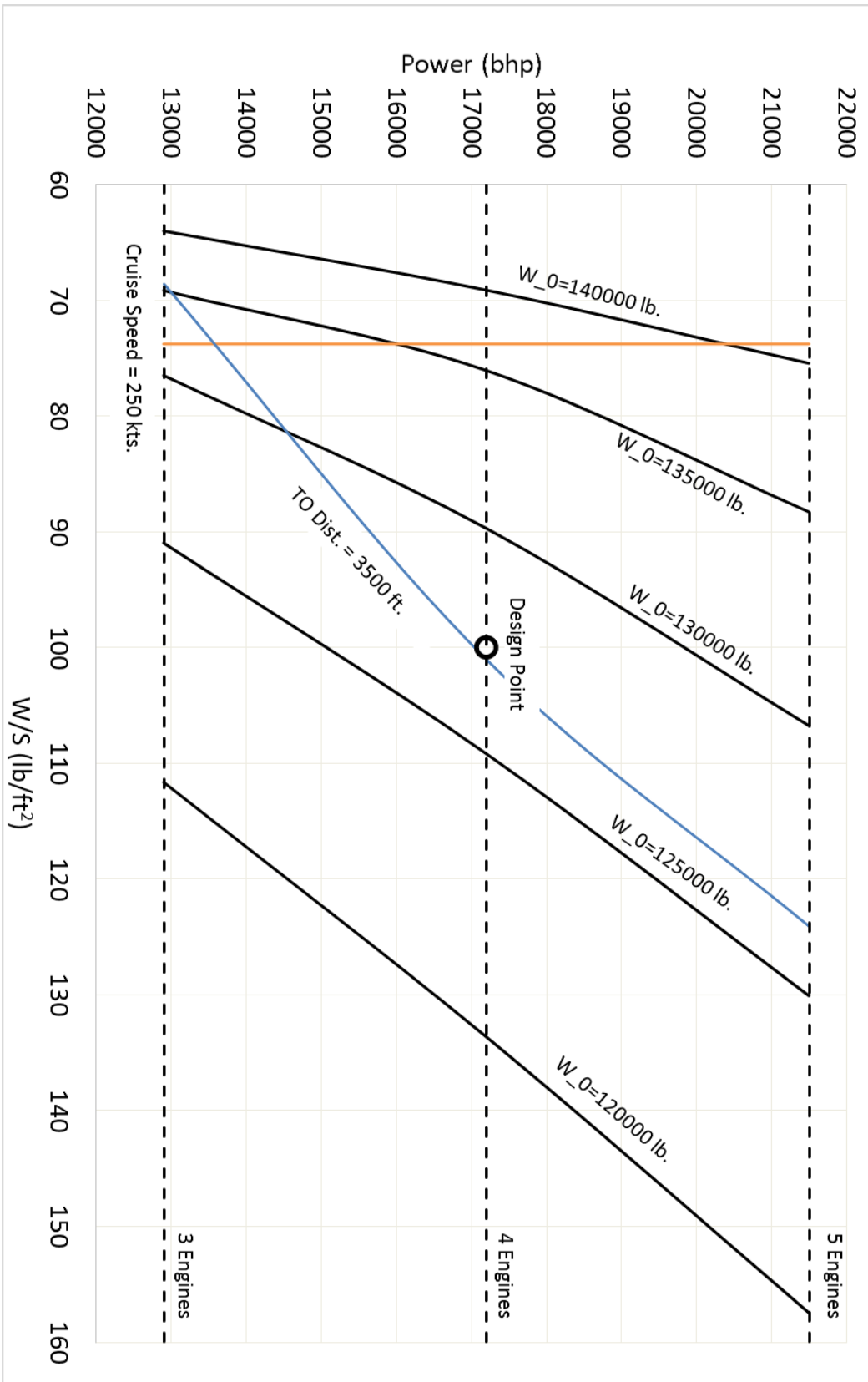




*Figure 22: Carpet plot of requirements and weights on a Power vs W/S graph.*

This plot serves to show two points. First of all it shows that the design is not possible with 3 engines only. That would violate the cruise speed requirement. Second, the design point shown corresponds to the lightest aircraft that fulfills all the requirements. This point is then chosen as the design point of the airplane and the aircraft was redesigned using the wing loading and power values of 100 lb/ft<sup>2</sup> and 17200 hp respectively. The resulting airplane dimensions and characteristics are given in CHAPTER 14.

Note that except for cruise speed and takeoff distance (shown as TO Dist.) all the other requirements were readily met and as such they were not included in the matrix plot.

# CHAPTER 12

## Additional Considerations

---

“I am well convinced that aerial navigation will form a most prominent feature in the progress of civilization.”

George Cayley

### 12.1 STABILITY AND CONTROL

#### 12.1.1 CG Envelope

For the aircraft to be stable at all times the aircraft CG has to stay within predefined limits. These limits are determined by calculating the maximum amount of moment that the horizontal tail can provide in either direction and leaving some margin for maneuverability. Furthermore the CG is not allowed to cross the neutral point because that would make the aircraft unstable. The following figure shows relative positions of the aircraft neutral point, aircraft CG, container CG and CG of the gates.

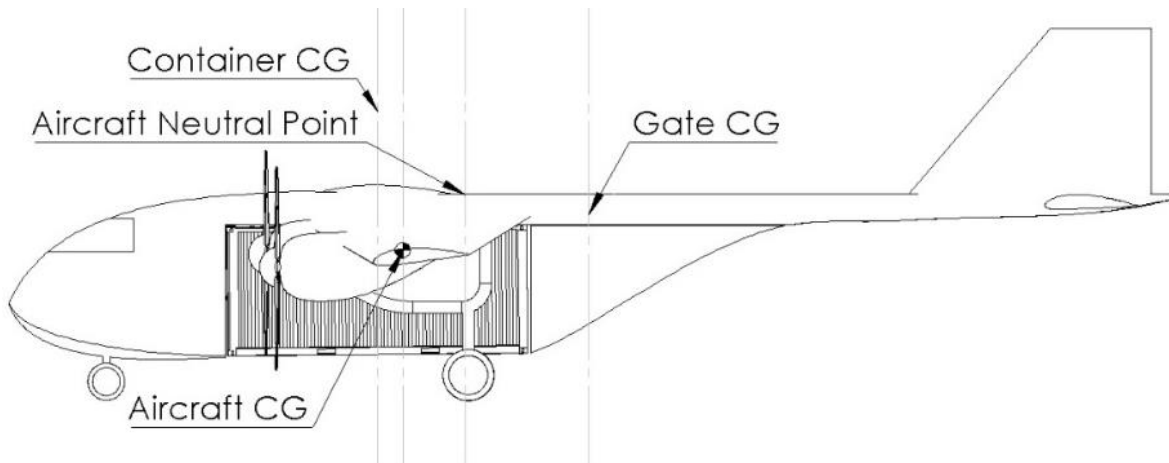


*Figure 23: Relative locations of some important points on Taj Pegasus.*

Note that the CG depicted here shows the location of CG before takeoff. Gate CG was approximated assuming the gates are homogenous sheet structures. Further, the container CG is assumed to be exactly at the middle of the container.

The container was intentionally placed slightly ahead of aircraft CG. This is because when containers are dropped or not loaded at all, the gates move forward. Even though the gates are not significantly heavy, the large displacement that they go through relatively large changes in CG location. As a result when the container is not present and the gates are in the forward position, the resulting aircraft CG is very close to the same as depicted in Figure 23.

Furthermore fuel tanks are almost exactly at the CG. This means the aircraft CG will be relatively fixed during the entire flight envelope and the aircraft will not experience serious changes in stability behavior.

The CG envelope of the aircraft is shown in Figure 24.

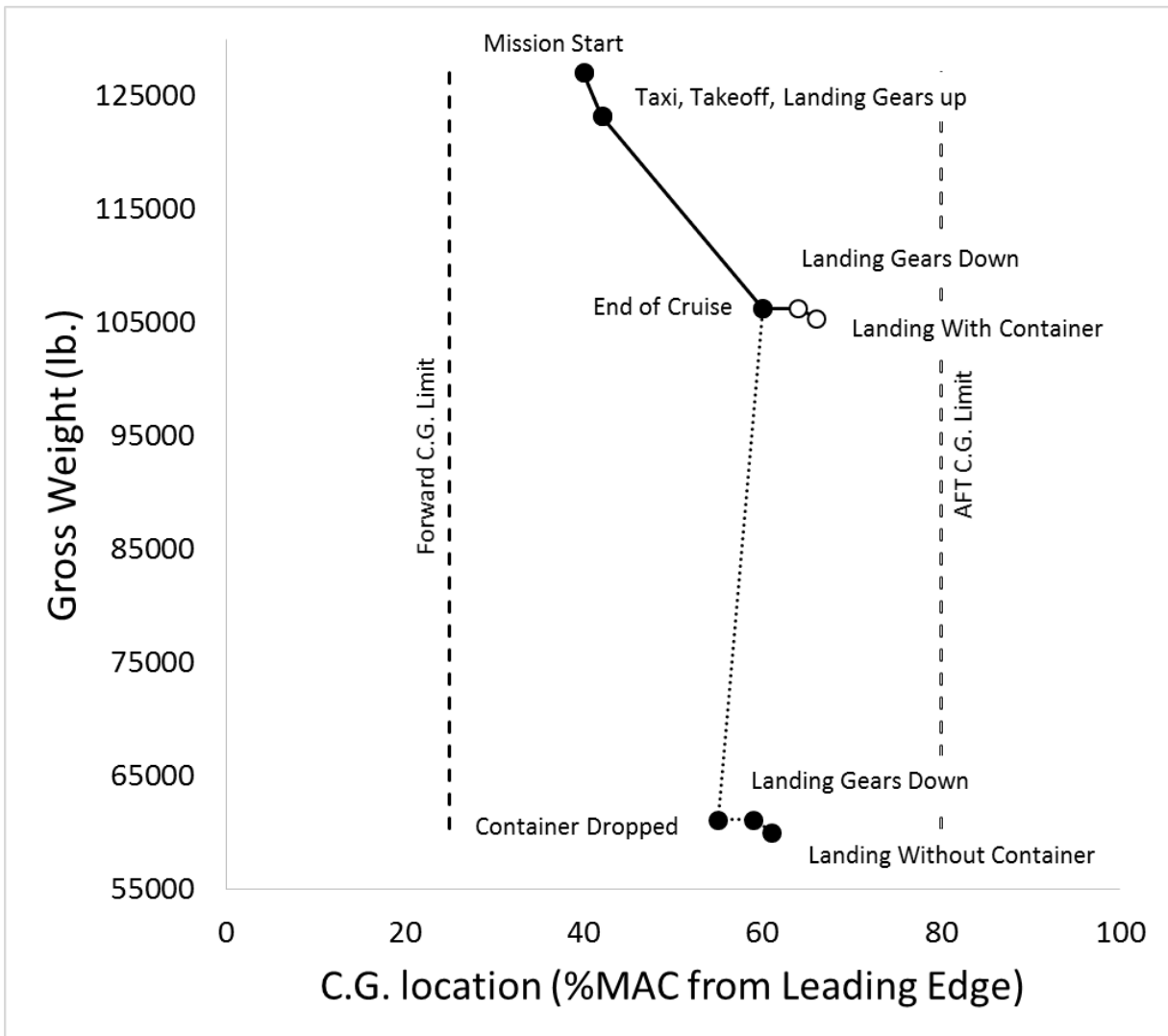


Figure 24: CG Envelope of Taj Pegasus for mission

### 12.1.2 Control Surfaces

A pair of ailerons and elevators and a rudder were placed on the aircraft. While designing the control surfaces they were made as long as possible. The ailerons were placed on the outboard portion of the wings and a small distance (0.5 ft) was left between the flap and the aileron so that a rib could pass between them. Similarly a small distance was left empty at the wing tip for another rib. The final length of each aileron is 17 ft.

Elevators and the rudder were placed such that they act on the entire span of the horizontal and vertical tail respectively.

The analysis of control surfaces is done in the using the vortex lattice method and it is explained in the following section.

### **12.1.3 Stability Derivatives**

During the early stages of aircraft design one of the best methods to determine the sensitivity of flight parameters to control surface inputs is the vortex lattice method. In this method a number of vortex sheets are placed on aircraft surfaces and the resulting aerodynamic forces and moments are calculated. The vortex lattice method program used in this report is called Athena Vortex Lattice (AVL) and it was developed in Massachusetts Institute of Technology [19]. The simplified model of Taj Pegasus in AVL and the summary of AVL output are given in Figure 25. Figure 26 shows sensitivity (derivative) of most relevant aerodynamic coefficients to flight conditions.

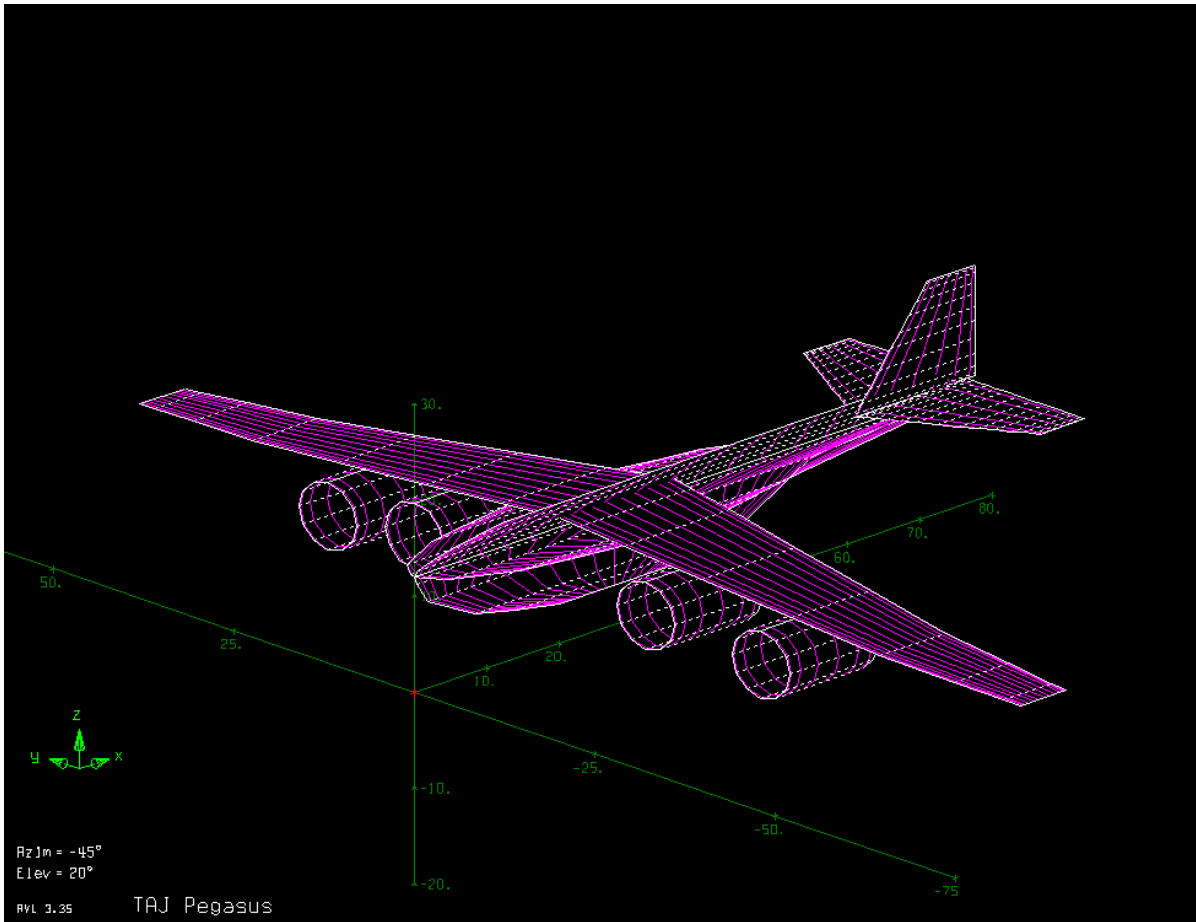


Figure 25: Simplified drawing of Taj Pegasus in AVL. Control surfaces are not shown here.

```

Stability-axis derivatives...
      alpha          beta
-----
z' force CL | CLa =  5.064899  CLb = -0.000000
y force CY | CYa = -0.000000  CYb = -0.858571
x' mom. Cl' | Cla = -0.000000  Clb =  0.005654
y mom. Cm | Cma = -1.819622  Cmb =  0.000002
z' mom. Cn' | Cna =  0.000000  Cnb =  0.086023

      roll rate p'      pitch rate q'      yaw rate r'
-----
z' force CL | CLp =  0.000000  CLq =  7.531145  CLr =  0.000000
y force CY | CYp =  0.089743  CYq =  0.000006  CYr =  0.136739
x' mom. Cl' | Clp = -0.533723  Clq =  0.000001  Clr =  0.105710
y mom. Cm | Cmp = -0.000000  Cmq = -22.420877  Cmr = -0.000001
z' mom. Cn' | Cnp = -0.050247  Cnq = -0.000003  Cnr = -0.047686

      LEflap      d1      flap      d2      aileron      d3      elevator      d4      rudder      d5
-----
z' force CL | CLd1 = -0.000701  CLd2 =  0.030196  CLd3 = -0.000000  CLd4 =  0.009584  CLd5 =  0.000000
y force CY | CYd1 = -0.000000  CYd2 = -0.000000  CYd3 = -0.000488  CYd4 = -0.000000  CYd5 = -0.000948
x' mom. Cl' | CLd1 =  0.000000  CLd2 =  0.000000  CLd3 =  0.002959  CLd4 = -0.000000  CLd5 = -0.000149
y mom. Cm | Cmd1 = -0.000271  Cmd2 = -0.002475  Cmd3 = -0.000000  Cmd4 = -0.035032  Cmd5 = -0.000000
z' mom. Cn' | Cnd1 = -0.000000  Cnd2 =  0.000000  Cnd3 = -0.000070  Cnd4 =  0.000000  Cnd5 =  0.000376
Treffz drag CDffd1 = -0.000020  CDffd2 =  0.000878  CDffd3 =  0.000000  CDffd4 =  0.000429  CDffd5 = -0.000000
span eff. | ed1 =  0.014128  ed2 = -0.619129  ed3 = -0.000000  ed4 = -0.368987  ed5 =  0.000000

```

Figure 26: Aerodynamic derivatives of Taj Pegasus taken from AVL output files.

For example the first data point at the top left, i.e. 5.064899 shows the derivative of coefficient of lift,  $C_L$  with respect to angle of attack,  $\alpha$ . Here axes  $x$ ,  $y$  and  $z$  are in the direction of aircraft nose, starboard wing tip and local gravitational vector respectively while  $x'$  and  $y'$  are in the direction of Lift force and starboard wing tip and  $z'$  is normal to these. While reading the data it is easy to confuse the direction of rotation. A control surface rotation that results in the aft of the surface going up is a positive rotation. For example leading edge flap may seem to be affecting coefficient of lift adversely, however this is not the case and the negative sign in front of the  $CLd1$  value should not confuse the readers. While reading the data it is easy to confuse the direction of rotation. A control surface rotation that results in the aft of the surface going up is a positive rotation. For example leading edge flap may seem to be affecting coefficient of lift adversely, however this is not the case and the negative sign in front of the  $CLd1$  value should not confuse the readers.

Note that despite being a simple method, AVL is a powerful tool. This can be verified by comparing its results with previously obtained data. For example lift curve slope was found to be  $C_{L\alpha} = 5.5$  in CHAPTER

9, AVL predicts a value of  $C_{La} = 5.064899$  which shows an error of only %10. Since this is a conceptual design only, the results of this program are deemed sufficient at this point.

## 12.2 HANDLING THE PAYLOAD

### 12.2.1 Attachment Mechanism

TAJ PEGASUS is required to swiftly pick up a 20 ft. container externally and deliver it to its destination. It is also required to drop the container mid-flight and fly without the container when desired. This requires additional aerodynamic and mechanical considerations in the design of the airplane. The containers have slots for hooks on all their corners. These slots are shown in Figure 27.

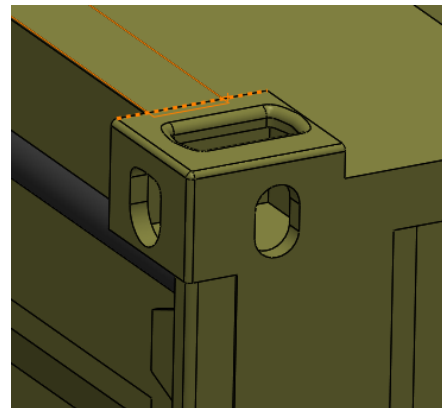


*Figure 27: Hook slots of the container.*

During the loading process the container will be moved on a truck from the rear side of the airplane until the two beams on the airplane are inserted into the two hook slots in the front of the container. Then the mechanical hooks are attached to the two hook slots in the back of the container. Now the container is fully constrained and attached to the airplane. During unloading on the ground this process is reversed.

When the container is to be released mid-air the mechanical hooks are simply opened. Since now the containers are not constrained at the back, and in the front they are just hanging on to two horizontal beams the container will quickly separate from the airplane and fall towards the ground.

### 12.2.2 Gates

TAJ PEGASUS has a set of two gate-like structures at the back that have the ability to move in two different manners. First the set of structures can open up to the sides. When the gates are in this position the



container can be moved to or from its loading position via a truck or by maneuvering the airplane itself. This process is depicted in Figure 28.

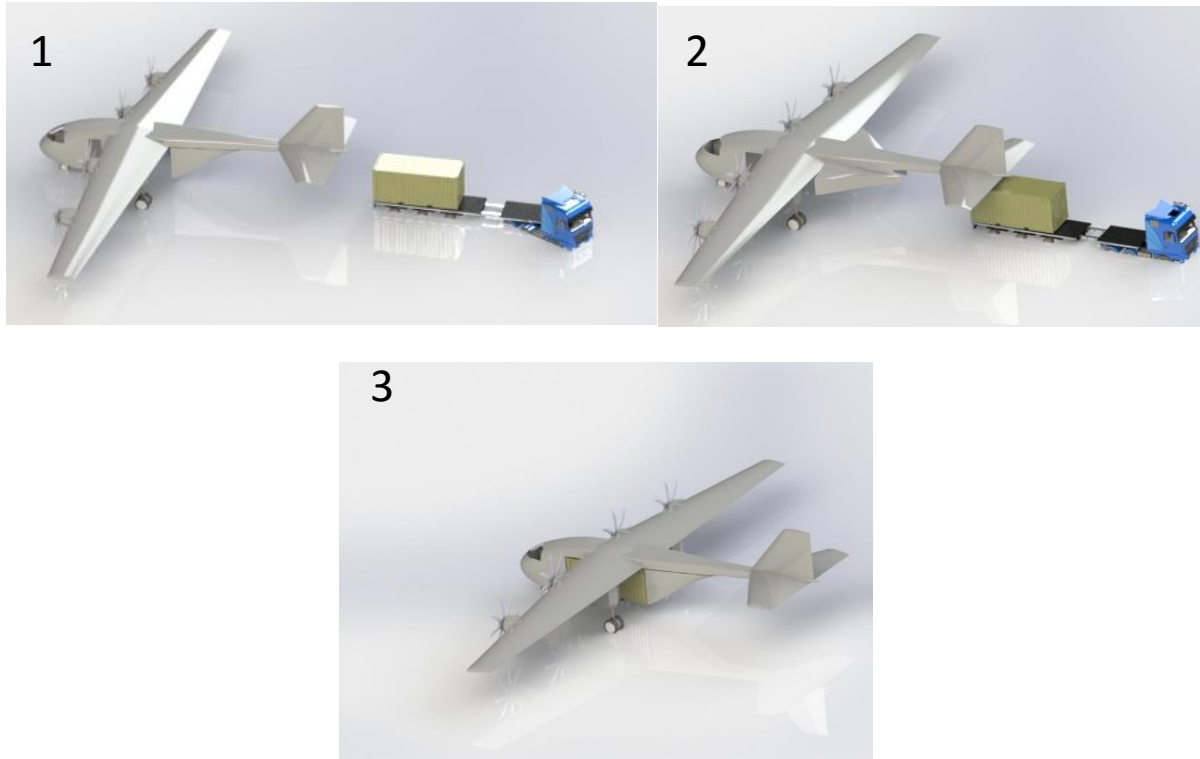


*Figure 28: Loading process of the container. Top left: The container has not been loaded yet. Top right: gates have opened and the container is now ready to be brought under the airplane. Bottom: The container is fully loaded and the gates have closed. During unloading this process is reversed.*

The second motion that the gates perform is longitudinal. The gates can move back and forth on the airplane. This is useful when the airplane is flying without the container. When moved forward, the gates close the rear of the crew station thus increasing aerodynamic efficiency of the airplane. This motion can be seen in the figures below.

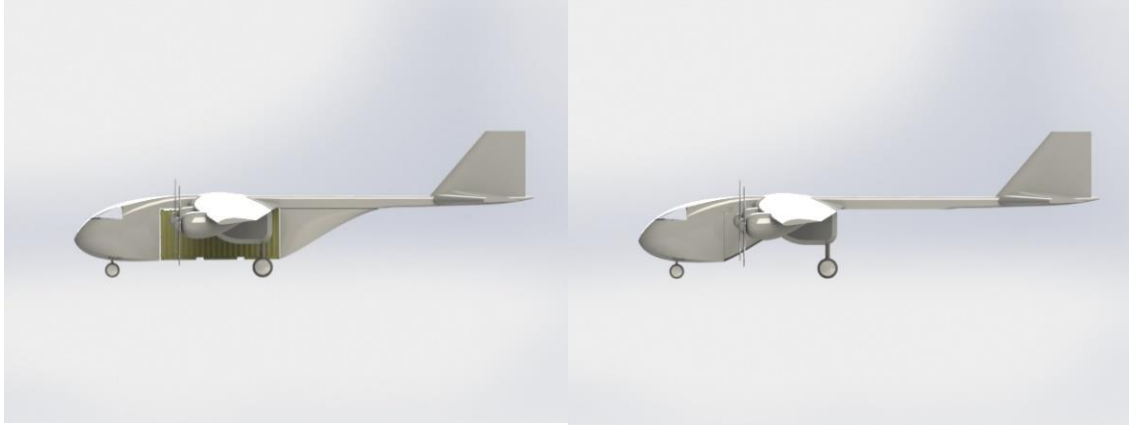


*Figure 29: Left: TAJ PEGASUS is ready to fly with the container. Right: The gates have moved forward and TAJ PEGASUS is ready to fly without the container.*

A combination of these two motions allows for dropping the container mid-air. While flying the gates are first opened up, the container is released using mechanical hooks, the gates close down and move forward to close the gap behind the crew station.

## 12.3 CREW STATION DESIGN

Crew station was designed to be as small as possible while still comfortably accommodating the crew. For a crew station with 3 crew members a length of 10.8 ft. is recommended [14]. This ensures that the crew members can comfortably stretch their legs, get up, and store their flight bags. The crew station of TAJ PEGASUS has a length of 10.8 ft. and height of 7.0 ft. at its maximum as seen from the photos below.

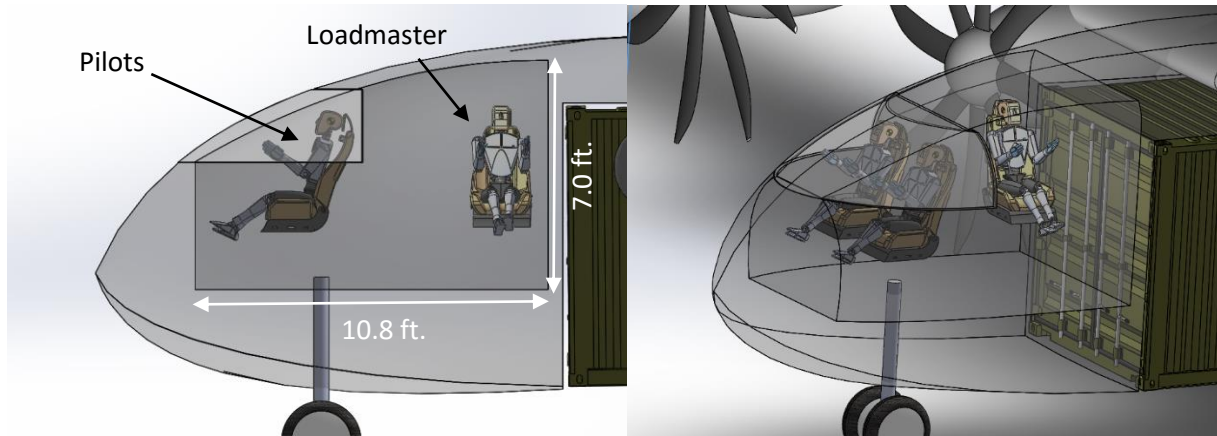


Figure 30: Crew station with two pilots and a loadmaster inside.

MIL-STD-850B defines vision requirements for various kinds of military aircraft. For military transport aircraft an over-nose angle of 17 deg. and over-side angle of 35 deg. are required [14]. The crew station of TAJ PEGASUS also complies with these requirements.

## 12.4 AIR LOADS AND STRUCTURES

Load factors (indicated by  $n$ ) are usually used to express the amount of loads that an aircraft is exposed to. For example  $n = 2$  means the aircraft is subjected to a load that is twice as much as its weight. As a result airplanes have limiting load factors that show the ultimate loads that the aircraft structures can carry. Typically transport airplanes are designed with positive load factor of 3 to 4 and negative load factor of -1 to -2. Taj Pegasus is designed with positive load factor of 3 and negative load factor of -2 [1]. The following V-n diagram was then obtained for this aircraft.

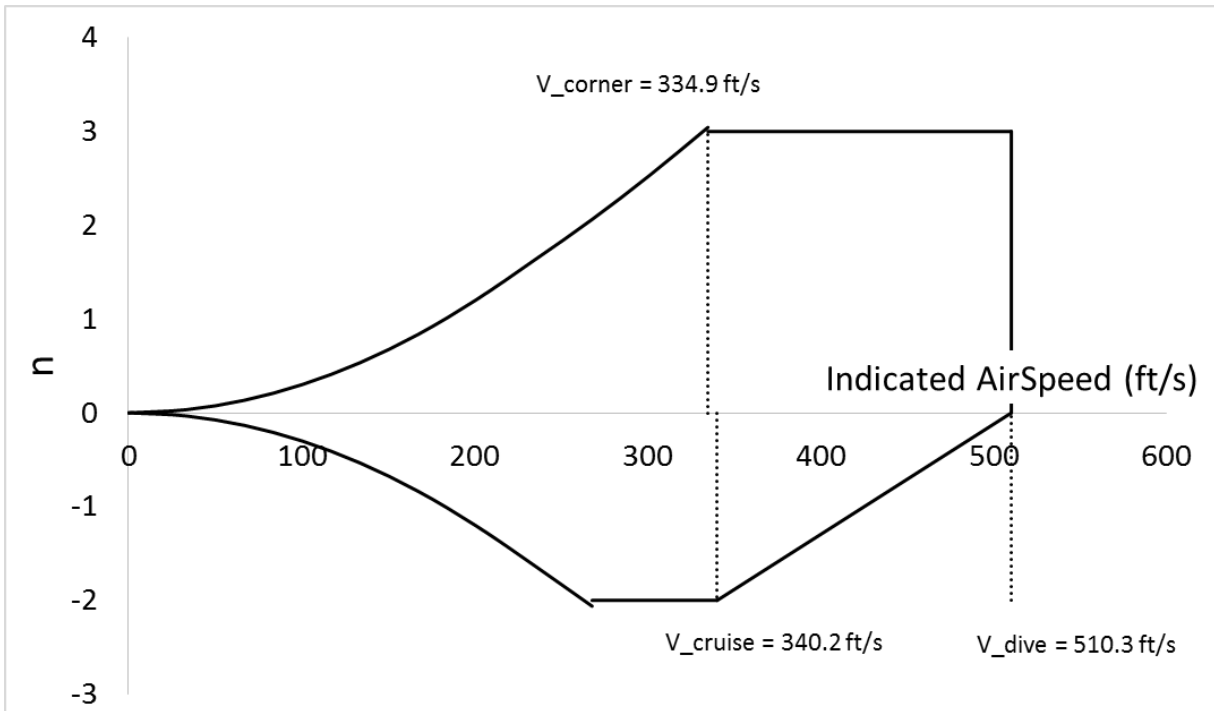


Figure 31: V-n diagram of Taj Pegasus.

The curved portions of the V-n diagram (to the left) are stall limits. The aircraft cannot cross those boundaries with those velocities. The horizontal lines at the top and bottom show the limiting load factors. And the vertical line to the right shows the dive speed. Aircraft structures can sustain only a limited amount of dynamic pressure and this line shows that limit.

Note that the V-n diagram is expressed in Indicated Air Speed (IAS). This is because using True Air Speed (TAS) would result in different V-n diagrams at different altitudes. However Figure 31 is valid at any altitude. Three most important velocities,  $V_{corner}$ ,  $V_{cruise}$  and  $V_{dive}$  are marked on the figure.  $V_{corner}$  is the smallest speed at which the aircraft can reach its limiting load factor and  $V_{dive}$  is the maximum speed the aircraft can reach. Also note that true cruise air speed of 450 ft/s was converted to the indicated airspeed before plotting the graph.

Gusts can have huge effects on the aircraft. They are often even more marked than maneuvers especially for transport aircraft. However when calculated gust loads were calculated it was observed that the

current limiting load factors are enough to sustain gusts at any speed and altitude. The following figure shows V-n diagram with gusts for reference.

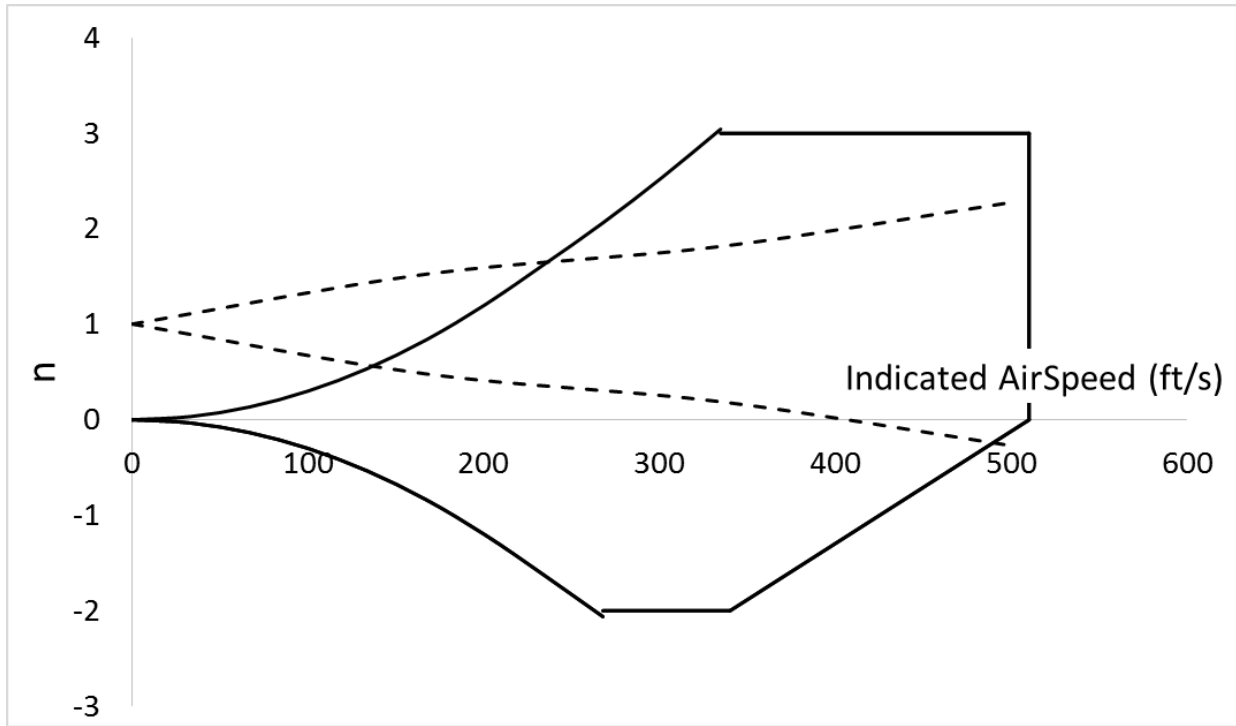
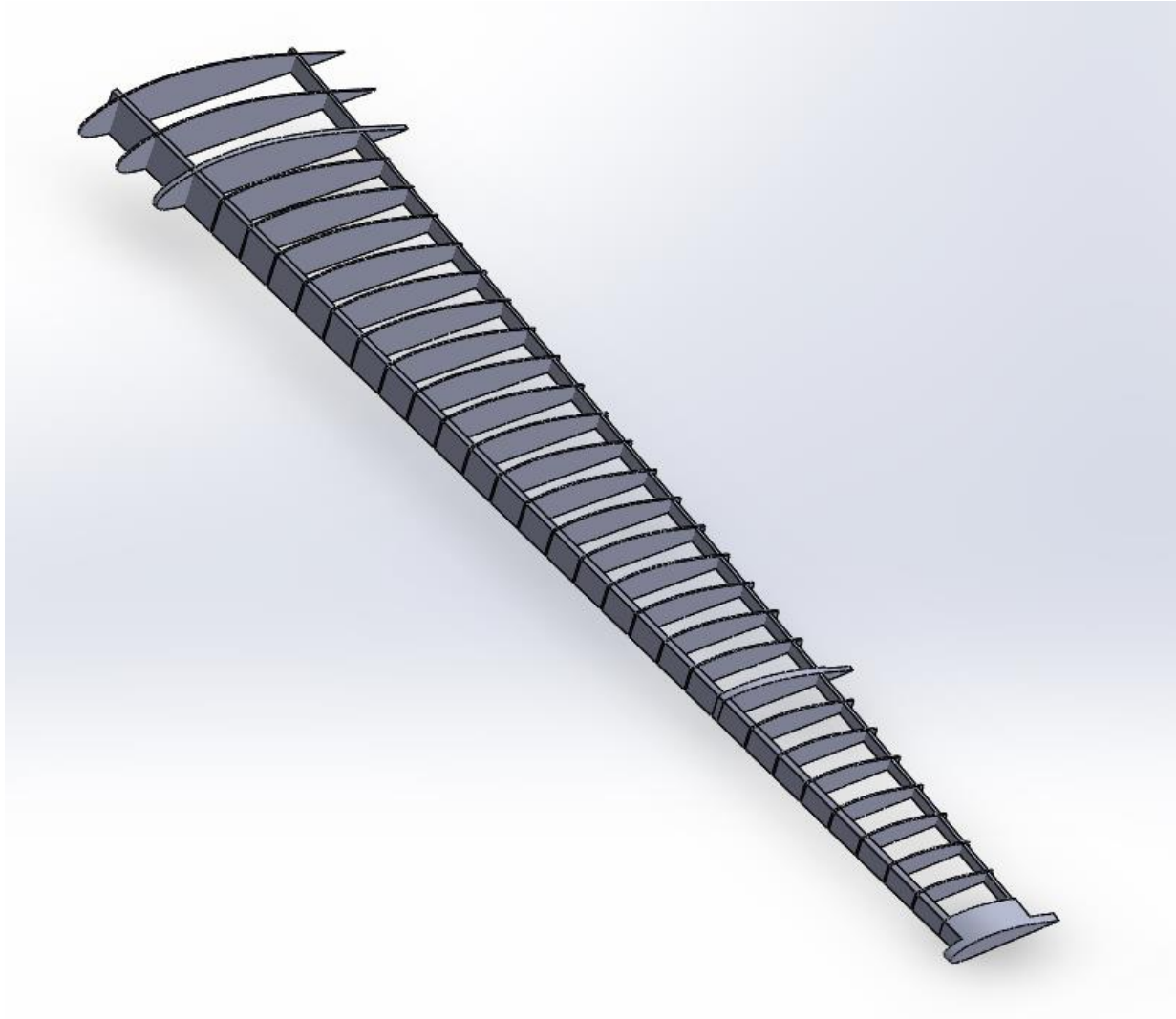


Figure 32: V-n diagram for Taj Pegasus. Note that the dashed lines show loads caused by gusts.

### 12.4.1 Wings

Wings will have a so called torque-box as the main load carrying component. The torque box is closed off by a front spar, a rear spar and upper and lower skins. Typical spar locations are 15-30 percent chord for front spar and 65-75 percent chord for rear spar. Wing ribs are usually about 24 in. apart in transport aircraft [20]. The leading edge flap spans throughout the wing however a small section of the wing leading edge (0.5 ft) was left empty near the fuselage and at the tip to allow wing ribs to pass through there. The flap encompasses about 38 ft of the wing span. The rest of the wing span is left for ailerons.



*Figure 33: Structural components of the wings.*

Figure 33 shows wing ribs and spars of Taj Pegasus. There are 30 spars spaced as evenly as possible and as close to the recommendations of [20] as possible. There are two spars that are at 25 and 70 percent of the chord line respectively.

### 12.4.2 Empennage

Typical spar locations for the empennage are 15-25 percent chord for front spar and 70-75 percent chord for rear spar. Ribs are about 24 in. apart as was the case in wings [20]. This information will be kept in mind while designing the structural members of the empennage.

### 12.4.3 Fuselage

Fuselage frames are usually  $0.02d_r+1$  in. and are spaced about 18-22 in. apart. Similarly longerons are usually 6-12 in. apart from each other in transport aircraft [20]. This information will be used when designing the structural members of the fuselage.

## 12.5 MATERIALS SELECTION

In the early years of aviation industry wood was extensively used in aircraft structures. This trend continued to some degree even to World War II. However by the end of the Second World War Aluminum, titanium and their alloys had completely replaced wood and its derivatives in aircraft structures. One of the most widely used Aluminum alloys, Aluminum 7075 (Aluminum, Copper, Magnesium, Zinc) will be used in the airframe of TAJ PEGASUS when needed. Aluminum 7075 has superior strength, even in the presence of cracks and it has a long fatigue life relative to other aluminum alloys [21].

Later in twentieth century composite materials, especially polymer-matrix composites reinforced with various fibers such as carbon and glass fibers started to be used in aviation industry. The contribution of composite materials in aircraft structures rapidly increased to the point that today about %25 of Lockheed Martin F-22 Raptor, %35 of the Joint Strike Fighter and %50 of Boeing 787 Dreamliner is made of composite materials [22], [23].

The main advantages of composite materials, especially Carbon Fiber Reinforced Plastics (CFRPs) include mass and part reduction, complex shape manufacturability, reduced scrap and improved fatigue life. While the main disadvantages to using them are high material and processing costs and low resistance to impact loading [24]. Especially high cost associated with composite materials was pronounced especially in the late twentieth century. For example according to 1980s estimates a kilogram of reduction in weight by using composite materials in large transport aircraft costed 300 USD [22]. However the latest trends in

the aerospace industry show that cost effectiveness of composite materials is increasing. This is very evident in the %50 share of composites in Boeing 787 as mentioned previously. The author of this report is also confident that cost effectiveness of composite materials will further increase until the time of production of TAJ PEGASUS. Based on this reasoning, composite materials will be used whenever possible.

### 12.5.1 Wings

Most structural components of the wings including all the spars and most ribs will be manufactured from CFRPs. There are some exceptions to this that are explained below.

The leading edge of the wings will be manufactured from aluminum 7075. The leading edge of a wing is very sensitive to surface roughness thus utmost importance should be given to the precision of manufacturing this part. Since CFRPs are not machineable their surface will not be as precise as a machined metal. Aluminum 7075 is used here because it is light and the loads that this part carries do not require very high strength. Another reason to use aluminum 7075 and not CFRP for this part is that, as mentioned before, CFRPs are weak in impact loading. The leading edge of the wing is the part that is most likely to receive impacts (such as accidental damage by the tools of technicians, bird collisions etc.) and using a CFRP here would be risky.

The two ribs connecting the wing to the fuselage will be made from titanium. The reason for this is high strength and ductility of titanium when compared to CFRPs. This part needs to be ductile because this part carries one of the greatest loadings in the wing and small flaws, cracks, dents and elongations of the part need to be detected swiftly to avoid material failures during flight. Since CFRPs are very brittle using them here could have disastrous consequences.



## 12.5.2 Fuselage

Just like wings most parts of the fuselage will be made from CFRPs. The exceptions to this are discussed below.

The nose cone will be made of Glass Fiber Reinforced Plastic (GFRP). This material allows for signals emitted from the radar to pass freely through it. The canopy will be made of acrylic as is done in most airplanes. Landing gear struts and hooks that will attach to the container will be made of steel. This is because other materials are simply not strong enough to support the loads applied on the struts. Finally the two gate-like structures behind the cockpit will be made of GFRP because GFRP is cheaper than CFRP and those parts do not carry major loads.

## 12.5.3 Tails

Almost the entirety of the structural members of the tails will be composed of CFRPs.

# CHAPTER 13

## Cost Analysis

“A billion here, a billion there – pretty soon it adds up to real money.”

Everett Mckinley Dirksen

The first step in estimating the cost of an airplane is to break it down into groups. The following figure obtained from [1] shows one such breakdown.

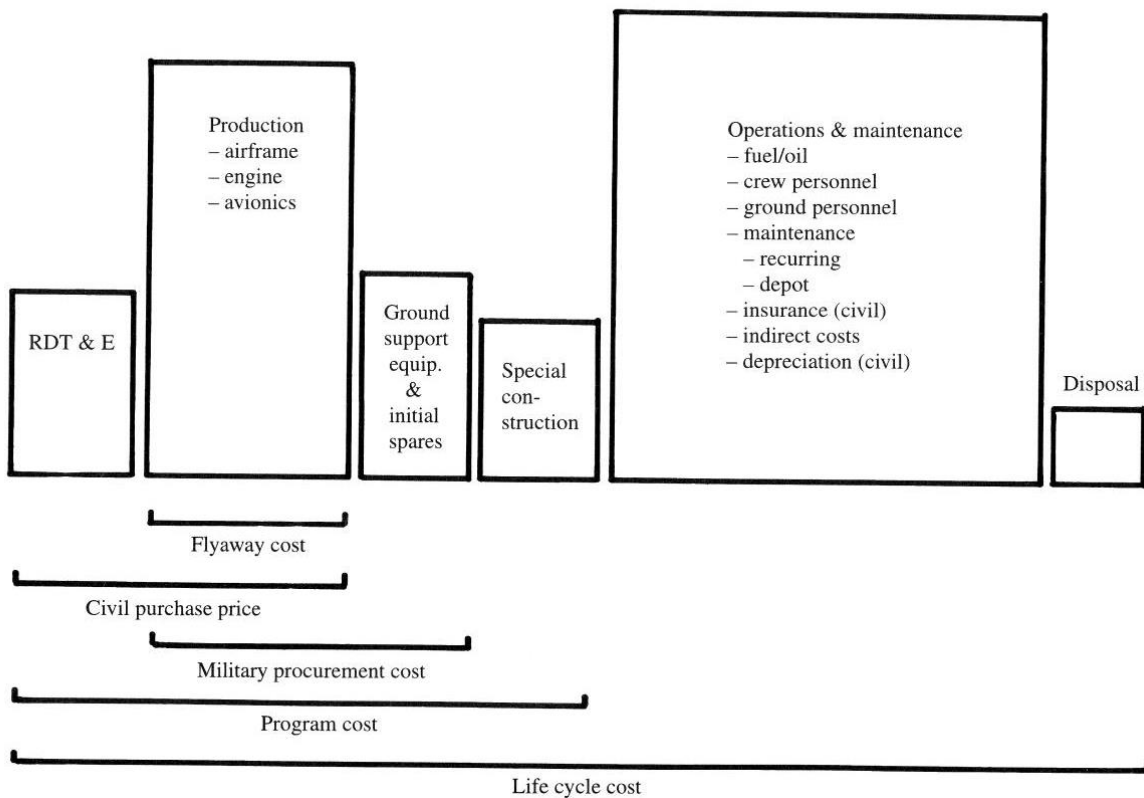


Figure 34: Elements of aircraft lifecycle cost.

The size of the boxes in Figure 34 are representative of approximate relative shares in total aircraft cost. Aircraft program starts with Research, Development, Test and Evaluation (RDT&E). This includes technology research, design engineering, prototype fabrication, flight and ground testing, and evaluations for operational suitability. The sum of RDT&E and flyaway costs are calculated in this report using DAPCA IV model. DAPCA stands for Development and Procurement Cost of Aircraft and it is a set of cost estimating relationships developed by RAND Corporation [1]. The model is rather simple but accurate results are obtained using this method. The model gives engineering, manufacturing, quality control and tooling hours based on aircraft empty weight, maximum speed and number to be built. The model also gives the cost for developing supporting infrastructure, flight test costs, and engineering production costs. These costs depend on empty weight, maximum velocity and number of flight test aircraft. The only area that DAPCA IV model falls short is the estimation of avionics cost.

Taj Pegasus has an empty weight of 59225.31 lb. and a maximum velocity of 386 kts. was calculated at sea level. It is assumed that only one flight test aircraft will be produced. Avionics of the aircraft was assumed to cost about 4000\$ per pound of aircraft empty weight. Rolls Royce Allison T-56 engine cost was around 3.19 million USD in 2014 [25].

DAPCA IV model is developed assuming the aircraft will be produced from aluminum. However some parts of Taj Pegasus are to be manufactured from Carbon Fiber Reinforced Polymers (CFRP), Glass Fiber Reinforced Polymers (GFRP) and titanium. To account for these a fudge factor of 1.2 was used.

An investment cost factor of 1.15 was used to allocate some contractor profit.

The sum of RDT&E and Flyaway costs are then presented below for a various production quantities. RDT&E and Flyaway costs per aircraft decrease as the production quantity increases. This is because the burden of RDT&E is distributed over more aircraft and the company producing the aircraft “learns” as it produces more and more aircraft.

Number of Aircraft Built	Total RDT&E + Flyaway cost (USD)	RDT&E + Flyaway Cost per Aircraft (USD)
1	1.81E+09	1.81E+09
10	3.10E+09	3.10E+08
20	3.85E+09	1.93E+08
30	4.43E+09	1.48E+08
40	4.93E+09	1.23E+08
50	5.37E+09	1.07E+08
60	5.78E+09	9.63E+07
70	6.15E+09	8.79E+07
80	6.51E+09	8.14E+07
90	6.85E+09	7.61E+07
100	7.17E+09	7.17E+07
110	7.48E+09	6.80E+07
120	7.77E+09	6.48E+07
130	8.06E+09	6.20E+07
140	8.34E+09	5.96E+07
150	8.61E+09	5.74E+07
160	8.88E+09	5.55E+07
170	9.13E+09	5.37E+07
180	9.39E+09	5.21E+07
190	9.63E+09	5.07E+07
200	9.87E+09	4.94E+07

*Figure 35: RDT&E and flyaway costs for various production quantities.*

Note that the cost estimates were done in constant 2016 dollars.

# CHAPTER 14

## Design Summary and Drawings

---

“A scientist discovers that which exists. An engineer creates that which never was.”

Theodore Von Karman

This document is the design report of TAJ PEGASUS, a transport aerial vehicle. The aircraft was designed in compliance with the Request for Proposal (RFP) published by American Institute of Aeronautics and Astronautics for the 2016 Individual Aircraft Design Competition. However the aircraft is not constrained to the mission specified in the RFP alone. Taj Pegasus could be used for various other missions as well. For example the container could be replaced with a radar and the aircraft could perform the role of Airborne Early Warning and Control aircraft. It could also be used as an intelligence gathering airplane in times of need because it has a large wing aspect ratio, low fuel consumption and high service ceiling. The removal of the container further adds to aerodynamic efficiency of the aircraft which helps it stay longer in the air.

Taj Pegasus could easily be employed in the commercial market as well. For example it could deliver aid in containers to regions hit by natural disasters. Scientific payloads could be installed instead of the container and weather, meteorology and geology studies could be performed. It would also be a great tool for cargo and transportation to remote areas since it can land and takeoff from rough surfaces.

The design started with a competitor study. The competitor study provided some initial ideas about the general layout, takeoff weight, wing span and area, aspect ratio and other aircraft parameters. The results of this study were used throughout the design process for comparison and determination of such parameters for this aircraft.

Competitor study was followed by an initial weight estimation. The method used here was a rather simple one with few inputs. As such the resulting weight estimate was crude, as seen in later stages of the design. Nevertheless the results of this estimate enabled predicting many design parameters such as wing loading.

Next an airfoil was selected for the aircraft. Some candidate airfoils were listed based on design coefficient of lift and cruise Mach number as criteria and the airfoil with the most desirable moment characteristics, maximum coefficient of lift and the coefficient of drag at design was selected for use in this aircraft. Other wing characteristics such as twist, sweep, dihedral, and taper ratio were also found using guidelines given in standard aircraft design books. The average aspect ratio of the competitor aircraft was used in this design.

Later two of the most critical performance parameters of an aircraft, power to weight ratio and wing loading were determined using the previous weight estimates. Determination of these was based on the type of the engine pre-specified in the Request for Proposal (RFP), competitor data and key performance requirements such as cruise, rate of climb, landing and takeoff distances and service ceiling. The largest wing loading that fulfills all of these requirements was then chosen to be used in this design.

The value for the weight of the aircraft was then estimated again using more advanced equations and more in-depth analysis than before. Wing loading and Power to weight ratio that were found in the previous chapter were used here to determine design takeoff weight of the aircraft, fuel weight and empty weight.

In CHAPTER 7 the geometry and shape of the largest components of the aircraft were determined. These include horizontal and vertical tails, wing and fuselage. Tail surface areas and moment arms were determined based on wing reference area using the historical trend equations found in aircraft design books. Wing reference area was found using the estimates of the design takeoff weight of the aircraft and wing loading obtained in the previous chapters. Fuselage length obtained using its empty weight. Fuel

volume was calculated using standard jet fuel properties and the fuel weight calculated in the previous chapter. Taj Pegasus was drawn using an open source 3D drawing package (OpenVSP) for the first time in this chapter and using SolidWorks in the later stages of the design.

In CHAPTER 8 the drawing was studied more closely and the location of the center of gravity was estimated. This estimate was later used to determine the location, type and tire width and radius of the landing gears. A more reliable estimate for aircraft weight was also obtained after summing weights of the individual components.

Aerodynamics of the aircraft was then investigated in detail in CHAPTER 9. High lift devices were chosen to be used in the aircraft. Lift curve slope and maximum coefficient of lift were calculated for clean and flapped configurations. The total parasite drag of the aircraft for different altitudes and flight regimes were determined using the component buildup method. Induced drag factor was found as a function of the aspect ratio of the aircraft. A plot of coefficient of lift versus angle of attack and a drag polar were then plotted and presented.

In CHAPTER 10 the performance of the aircraft was measured and compared to the key performance requirements. It was verified that all the requirements are met.

An optimization was done on Taj Pegasus and the optimum wing loading and power were obtained from a carpet plot. The aircraft was then redesigned with the new parameters.

Finally various subjects like structures, stability and control were addressed in the final chapter.

Some pictures of Taj Pegasus followed by a table of key characteristics is given below.

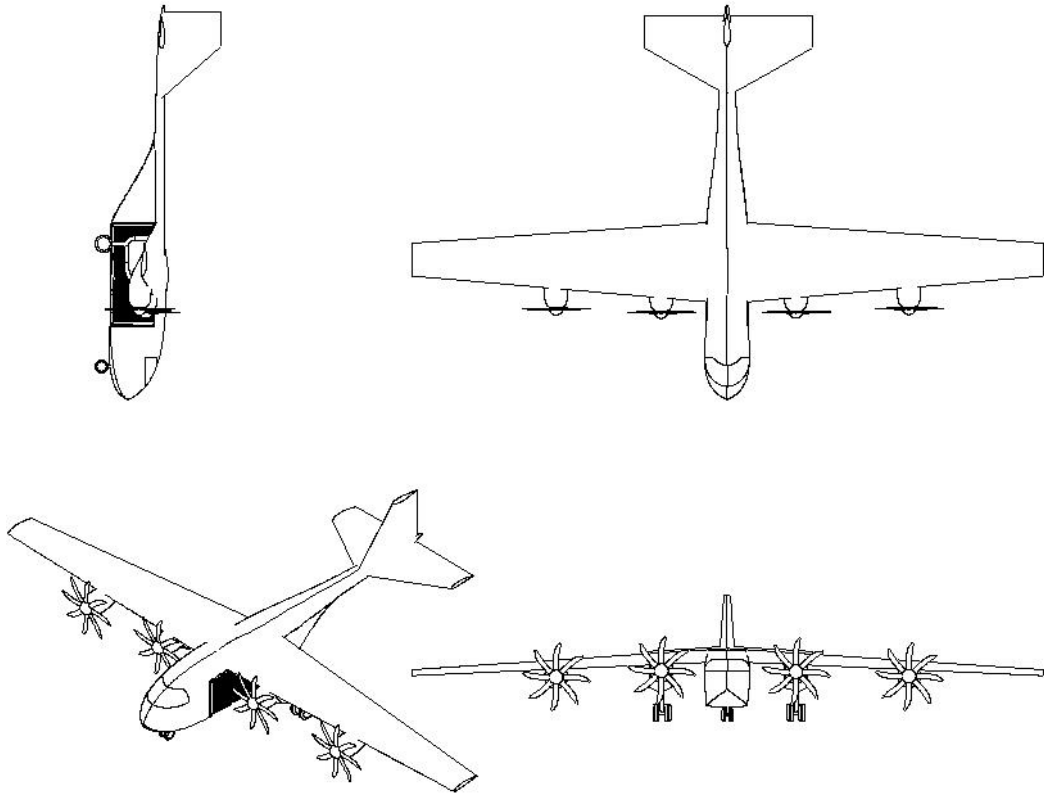


Figure 36: A three view image of TAJ PEGASUS.





*Figure 37: An isometric view of TAJ PEGASUS.*



*Figure 38: An isometric view of Taj Pegasus when the container is removed.*



*Figure 39: Front view of Taj Pegasus.*

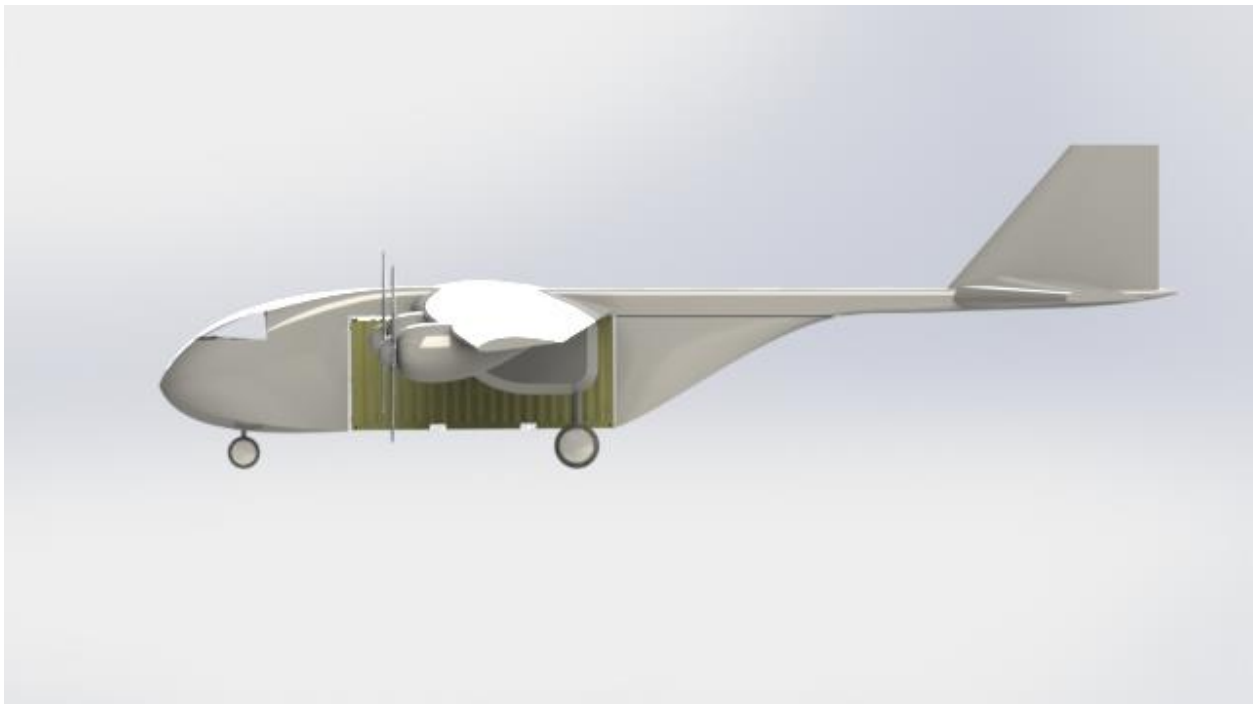


*Figure 40: Side view of Taj Pegasus.*

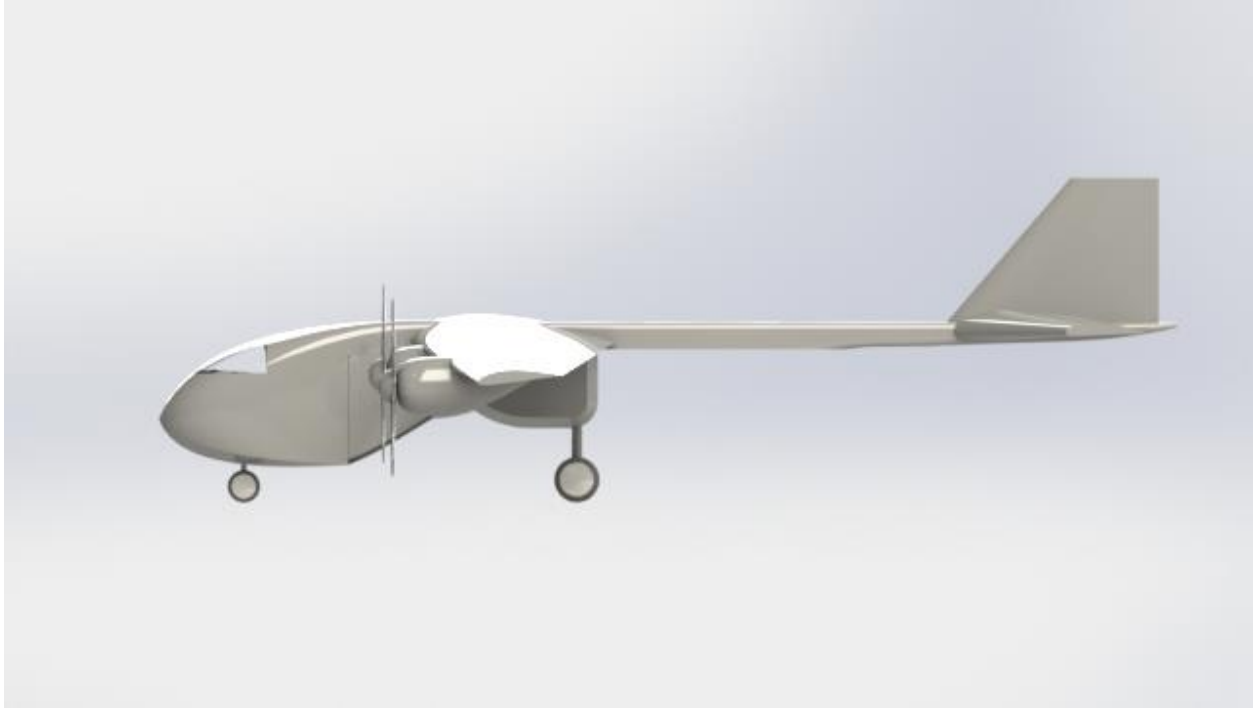


*Figure 41: Side view of Taj Pegasus when the container is removed.*



*Figure 42: Top view of Taj Pegasus.*

<b>Length (overall)</b>	80 ft
<b>Height (overall)</b>	30 ft
<b>Design Takeoff Weight</b>	127058.7 lb
<b>Empty Weight</b>	59255.3 lb
<b>Fuel Weight</b>	22063.4 lb
<b>Wing Span</b>	120.5 ft
<b>Wing Area</b>	1319.1 ft <sup>2</sup>
<b>Wing Aspect Ratio</b>	10.98
<b>Propeller Diameter</b>	13.5 ft
<b>Cruise Speed</b>	490 ft/s (290.3 knots)
<b>Rate of Climb at 10000 ft</b>	3493.2 ft/min
<b>Range</b>	1327.5 nm
<b>Takeoff Distance</b>	3500 ft
<b>Landing Distance</b>	3103.1 ft
<b>Service Ceiling (With empty container)</b>	47300 ft
<b>Power Plant</b>	Rolls Royce Allison T-56-A-15
<b>Number of Engines</b>	4

*Figure 43: Key parameters and dimensions of TAJ PEGASUS.*

# REFERENCES:

- [1] D. P. Raymer, *Aircraft Design: A Conceptual Approach*, 2nd ed. Washington, DC: American Institute of Aeronautics and Astronautics, Inc., 1992.
- [2] "Atmospheric Properties Calculator," *Aerospaceweb.org*, 2016. [Online]. Available: <http://www.aerospaceweb.org/design/scripts/atmosphere/>. [Accessed: 05-Apr-2016].
- [3] "Alenia C-27J Spartan," *AxleGeeks*, 2015. [Online]. Available: <http://planes.axlegeeks.com/l/158/Alenia-C-27J-Spartan>. [Accessed: 20-Sep-2015].
- [4] "Antonov An-12," *Aeromarine International*. [Online]. Available: <http://www.aeromarine.com/An-12.pdf>. [Accessed: 20-Sep-2015].
- [5] G. Goebel, "The Antonov an-12," *Airvectors*, 2014. [Online]. Available: <http://www.airvectors.net/avan12.html>. [Accessed: 20-Sep-2015].
- [6] "C-123 Provider," *Global Aircraft*. [Online]. Available: [http://www.globalaircraft.org/planes/c-123\\_provider.pl](http://www.globalaircraft.org/planes/c-123_provider.pl). [Accessed: 20-Sep-2015].
- [7] "Eurocontrol Training Zone." [Online]. Available: <http://contentzone.eurocontrol.int/>. [Accessed: 20-Sep-2015].
- [8] P. Jackson, *Jane's All the world's aircraft 2009-2010*. Jane's Information Group, 2010.
- [9] "Kawasaki C-1," *Onwar.com*, 2015. [Online]. Available: [https://www.onwar.com/weapons/aircraft/planes/Kawasaki\\_C1.html](https://www.onwar.com/weapons/aircraft/planes/Kawasaki_C1.html). [Accessed: 20-Sep-2015].
- [10] K. Palt, "Flugzeug," 2015. [Online]. Available: <http://www.flugzeuginfo.net/>. [Accessed: 20-Sep-2015].
- [11] J. Pike, "C-130J specifications and performance," *GlobalSecurity*, 2011. [Online]. Available: <http://www.globalsecurity.org/military/systems/aircraft/c-130j-specs.htm>. [Accessed: 20-Sep-2015].
- [12] "Transall C-160," *All-aero.com*, 2014. [Online]. Available: <http://all-aero.com/index.php/contactus/55-planes-t-u/8098-transall-c-160>. [Accessed: 20-Sep-2015].
- [13] J. John D. Anderson, *Aircraft Performance and Design*, 1st ed. McGraw-Hill Companies, Inc., 1999.
- [14] L. M. Nicolai, G. E. Carichner, J. A. Schetz, and L. M. L. Malcolm, *Fundamentals of Aircraft and Airship Design*, vol. I. Reston, Virginia: American Institute of Aeronautics and Astronautics, Inc., 2010.
- [15] "Atmosphere Properties," *Rocket & Space Technology*. [Online]. Available: <http://www.braeunig.us/space/atmos.htm>. [Accessed: 18-Nov-2015].
- [16] "Speed of Sound at Different Altitudes," *Fighter Planes and Military Aircraft*, 2011. [Online]. Available: <http://www.fighter-planes.com/jetmach1.htm>. [Accessed: 08-Nov-2015].
- [17] "GLOSSARY OF DEFINITIONS, GROUND RULES, AND MISSION PROFILES TO DEFINE AIR VEHICLE

PERFORMANCE CAPABILITY," *MIL-STD-3013*, 2003.

- [18] S. F. Hoerner, *Fluid-Dynamic Drag; Practical Information on Aerodynamic Drag and Hydrodynamic Resistance*. Bakersfield, CA: Hoerner Fluid Dynamics, 1965.
- [19] M. Drela and H. Youngren, "AVL Overview," *MIT*, 2015. [Online]. Available: <http://web.mit.edu/drela/Public/web/avl/>. [Accessed: 24-Mar-2016].
- [20] J. Roskam, "Airplane Design," in *Part III: Layout Design of Cockpit, Fuselage, Wing and Empennage: Cutaways and Inboard Profiles*, Ottawa, Kansas: Roskam Aviation and Engineering Corporation, 1989.
- [21] M. C.-Y. Niu, *Airframe Structural Design*. Los angeles, California: Technical Book Company, 1988.
- [22] A. Baker, S. Dutton, and D. Kelly, *Composite Materials for Aircraft Structures*, 2nd ed. Reston, Virginia: American Institute of Aeronautics and Astronautics, Inc., 2004.
- [23] "Boeing 787 From The Ground Up," *AERO*, 2006. [Online]. Available: [http://www.boeing.com/commercial/aeromagazine/articles/qtr\\_4\\_06/AERO\\_Q406.pdf](http://www.boeing.com/commercial/aeromagazine/articles/qtr_4_06/AERO_Q406.pdf). [Accessed: 09-Mar-2016].
- [24] C. Æ. Soutis, "Fibre reinforced composites in aircraft construction," vol. 41, pp. 143–151, 2005.
- [25] "Contracts," *Department of Defense*, 2016. [Online]. Available: <http://www.defense.gov/News/Contracts>.